nents of NADPH oxidase activation, the origin of PTX-induced ROS production may be NADPH oxidase. In addition, PTX induced degradation of IκBα proteins in a time-dependent manner, which was abolished by Rac inhibition (supplemental Fig. 3). Although molecular mechanism underlying ROS-mediated NF-κB activation is still unknown, this result implies that ROS-mediated inhibition of mitogen-activated protein kinase phosphatases may be involved (60). Because the promoter regions of IL-1β and AT1R contain a putative NF-κB binding site, AT1R up-regulation may be induced by direct interaction of AT1R promoter with NF-κB. However, PTX-induced enhancement of Ca^{2} response by AT1R stimulation was almost completely suppressed by anti-IL-1β antibody and IL-1β siRNAs (Fig. 2). Thus, IL-1β released from fibroblasts by PTX treatment may be the main mechanism of PTX-induced AT1R up-regulation. Furthermore, Rac1 inhibition suppressed PTX-induced IL-1β production, and IL-1β inhibition suppressed PTX-induced Rac activation at a late but not an early phase (Fig. 6). Thus, Rac-mediated IL-1β production may amplify Rac-dependent signaling through IL-1β-mediated Rac activation. These results suggest that PTX induces AT1R up-regulation through a TLR4 → PI 3-kinase → Rac → NADPH oxidase → ROS → NF-κB → IL-1β-dependent signal pathway (Fig. 8).

We revealed that stimulation of TLR4 mediates PTX-induced AT1R up-regulation. It is thought that MyD88 and Trif-related adaptor molecule mediate TLR4-mediated NF-κB activation (32). However, it has recently been reported that oxidized LDL induces NADPH oxidase-dependent ROS production through TLR4 stimulation in macrophages (59). These authors have also demonstrated that Syk but not MyD88 is responsible for TLR4-mediated ROS production. In addition, another study has shown that stimulation of TLR4 by PTX B-oligomer induces activation of MyD88-independent signaling pathways (10). Thus, PTX induces stimulation of TLR4 that preferentially activates the Syk-dependent Rac signaling pathway.

PTX is frequently used as a specific tool to examine the involvement of G_i in cellular signaling. Abolishment of TLR4 by siRNA did not affect PTX-mediated ADP-ribosylation of G_i and G_o (Fig. 7*D*). Thus, PTX binds to two receptors; one is TLR4 that activates Rac and another is the binding site that liberates the A-protomer into cells. So far, the G_i/G_o-independent signaling pathway is not usually considered when PTX is used *in vitro* and *in vivo*. Because PTX activates Rac in addition to ADP-ribosylation of G_i and G_o, it is no longer thought that PTX is a specific inhibitor of receptor-G_i signaling.

Another important finding of this study is that Rac is a physiological mediator of AT1R up-regulation induced by IL-1β stimulation. The inhibition of Rac suppressed the increase in AT1R density and the enhancement of Ang II-induced Ca^{2+} response by IL-1β stimulation (Fig. 6 and supplemental Fig. 4). Because other agonists that up-regulate AT1R, such as Ang II and TNF-α, also increase Rac activity, Rac-mediated AT1R up-regulation may be a common mechanism among various stimuli. Statins are inhibitors of 3-hydroxy-3-methylglutaryl-CoA reductase and appear

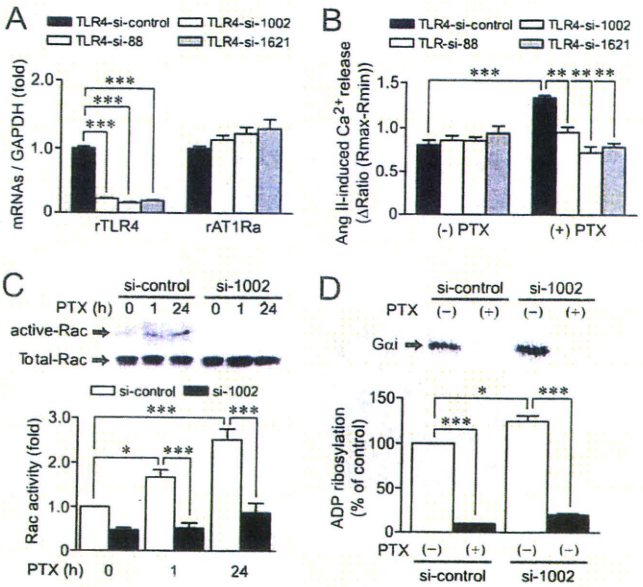

FIGURE 7. **Roles of TLR4 in PTX-induced Rac activation and ADP-ribosylation of G_i/G_o.** *A*, effects of TLR4 siRNAs on the expression of TLR4 and AT1R mRNAs. *B*, effects of TLR4 siRNAs on PTX-induced enhancement of Ang II-induced Ca^{2+} responses. Cells were treated with PTX for 24 h after siRNA treatment for 48 h. *C*, effects of TLR4 siRNA (si-1002) on PTX-induced Rac activation. *D*, effects of TLR4 siRNA on PTX-induced ADP-ribosylation of $G\alpha_i$ proteins. *, $p < 0.05$; **, $p < 0.01$; ***, $p < 0.001$. *Error bars*, S.E.

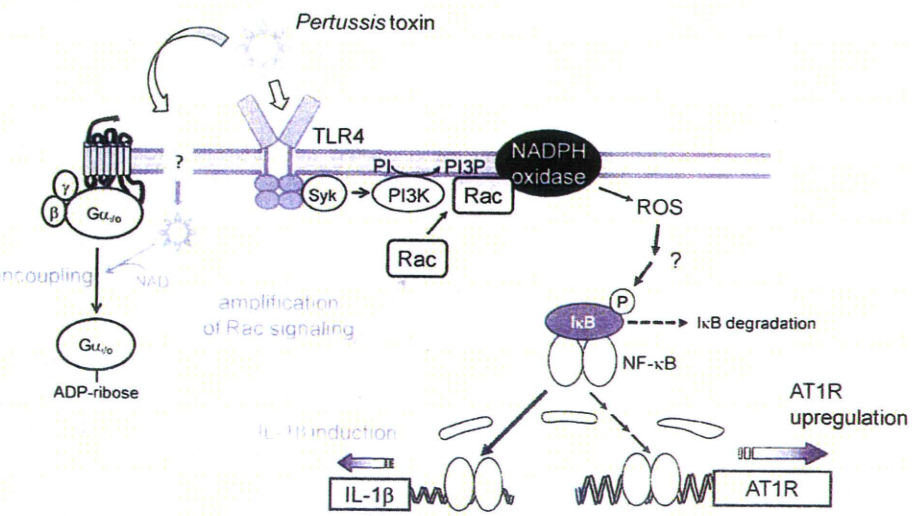

FIGURE 8. **Schema of TLR4-mediated AT1R up-regulation induced by PTX.** PTX induces ROS production through sequential activation of TLR4, Syk, PI 3-kinase (*PI3K*), Rac, and NADPH oxidase. Although the mechanism of NF-κB activation induced by ROS is still unknown, ROS mediate NF-κB-dependent expression of IL-1β. Induction of IL-1β also induces Rac activation through IL-1 receptor stimulation, leading to amplification of Rac-dependent signaling. Sustained activation of Rac may be required for PTX-induced AT1R up-regulation in rat cardiac fibroblasts. A-protomer of PTX enters the cells through unidentified binding site, and ADP-ribosylates G_i/G_o proteins.

to have pleiotropic effects on the cardiovascular system that are independent of their ability to decrease serum cholesterol (14, 55). These include inhibition of cardiac hypertrophy and left ventricular dysfunction, anti-inflammatory effects, and antioxidative effects (55, 61). Recent studies have demonstrated that statins inhibit ROS production and myocardial apoptosis by inhibition of Rac (57). Up-regulation of AT1R is thought to be one of the features involved in cardiac remodeling. Thus, the present results suggest a novel mechanism in which statins inhibit cardiac fibrosis by inhibition of AT1R up-regulation in cardiac fibroblasts. Statins also inhibit Rho activity by inhibition of isoprenylation. However, we could not detect the activation of Rho, Ras, and Rap1 by PTX treatment (supplemental Fig. 2). Thus, inhibition of Rac is essential for the inhibition of AT1R up-regulation by statin.

In conclusion, we demonstrated a novel action of PTX that induces AT1R up-regulation independently of ADP-ribosylation of G_i/G_o. This mechanism includes TLR4-mediated Rac activation, ROS production, and NF-κB activation. Activation of NF-κB induces IL-1β production, resulting in amplification of Rac signaling, which leads to increase in AT1R density. The involvement of the TLR4-Rac signaling pathway in the regulation of AT1R density will provide a possible novel target for inhibiting cardiac remodeling. In addition, we have provided pharmacologically important information indicating that PTX *per se* influences G protein-coupled receptor signaling independently of $G\alpha_i$ inhibition. Activation of the TLR4-Rac signaling pathway by PTX suggests that we should consider pharmacological actions of PTX in addition to a specific inhibitor of G_i/G_o-mediated signal transduction.

Acknowledgment—We thank Miyuki Toyotaka for analyzing the localization of the NF-κB p65 subunit.

REFERENCES

1. Katada, T., and Ui, M. (1982) *J. Biol. Chem.* **257,** 7210–7216
2. Kurose, H., Katada, T., Amano, T., and Ui, M. (1983) *J. Biol. Chem.* **258,** 4870–4875
3. Tamura, M., Nogimori, K., Yajima, M., Ase, K., and Ui, M. (1983) *J. Biol. Chem.* **258,** 6756–6761
4. Lando, Z., Teitelbaum, D., and Arnon, R. (1980) *Nature* **287,** 551–552
5. Linthicum, D. S., Munoz, J. J., and Blaskett, A. (1982) *Cell Immunol.* **73,** 299–310
6. Racke, M. K., Hu, W., and Lovett-Racke, A. E. (2005) *Trends Immunol.* **26,** 289–291
7. Jajoo, S., Mukherjea, D., Pingle, S., Sekino, Y., and Ramkumar, V. (2006) *J. Pharmacol. Exp. Ther.* **317,** 1–10
8. Li, H., and Wong, W. S. (2001) *Biochem. Biophys. Res. Commun.* **283,** 1077–1082
9. Melien, O., Sandnes, D., Johansen, E. J., and Christoffersen, T. (2000) *J. Cell Physiol.* **184,** 27–36
10. Wang, Z. Y., Yang, D., Chen, Q., Leifer, C. A., Segal, D. M., Su, S. B., Caspi, R. R., Howard, Z. O., and Oppenheim, J. J. (2006) *Exp. Hematol.* **34,** 1115–1124
11. Timmermans, P. B., Wong, P. C., Chiu, A. T., Herblin, W. F., Benfield, P., Carini, D. J., Lee, R. J., Wexler, R. R., Saye, J. A., and Smith, R. D. (1993) *Pharmacol. Rev.* **45,** 205–251
12. de Gasparo, M., Catt, K. J., Inagami, T., Wright, J. W., and Unger, T. (2000) *Pharmacol. Rev.* **52,** 415–472
13. Onohara, N., Nishida, M., Inoue, R., Kobayashi, H., Sumimoto, H., Sato, Y., Mori, Y., Nagao, T., and Kurose, H. (2006) *EMBO J.* **25,** 5305–5316
14. Brown, R. D., Ambler, S. K., Mitchell, M. D., and Long, C. S. (2005) *Annu. Rev. Pharmacol. Toxicol.* **45,** 657–687
15. Villarreal, F. J., Kim, N. N., Ungab, G. D., Printz, M. P., and Dillmann, W. H. (1993) *Circulation* **88,** 2849–2861
16. Sakata, Y., Hoit, B. D., Liggett, S. B., Walsh, R. A., and Dorn, G. W., 2nd (1998) *Circulation* **97,** 1488–1495
17. Gurantz, D., Cowling, R. T., Varki, N., Frikovsky, E., Moore, C. D., and Greenberg, B. H. (2005) *J. Mol. Cell Cardiol.* **38,** 505–515
18. Nio, Y., Matsubara, H., Murasawa, S., Kanasaki, M., and Inada, M. (1995) *J. Clin. Invest.* **95,** 46–54
19. Yamani, M. H., Cook, D. J., Tuzcu, E. M., Abdo, A., Paul, P., Ratliff, N. B., Yu, Y., Yousufuddin, M., Feng, J., Hobbs, R., Rincon, G., Bott-Silverman, C., McCarthy, P. M., Young, J. B., and Starling, R. C. (2004) *Am. J. Transplant.* **4,** 1097–1102
20. Peng, J., Gurantz, D., Tran, V., Cowling, R. T., and Greenberg, B. H. (2002) *Circ. Res.* **91,** 1119–1126
21. Finkel, T. (1999) *J. Leukoc. Biol.* **65,** 337–340
22. Griendling, K. K., and Ushio-Fukai, M. (2000) *Regul. Pept.* **91,** 21–27
23. Sundaresan, M., Yu, Z. X., Ferrans, V. J., Sulciner, D. J., Gutkind, J. S., Irani, K., Goldschmidt-Clermont, P. J., and Finkel, T. (1996) *Biochem. J.* **318,** 379–382
24. Sumimoto, H. (2008) *FEBS J.* **275,** 3249–3277
25. Sulciner, D. J., Irani, K., Yu, Z. X., Ferrans, V. J., Goldschmidt-Clermont, P., and Finkel, T. (1996) *Mol. Cell Biol.* **16,** 7115–7121
26. Nishida, M., Tanabe, S., Maruyama, Y., Mangmool, S., Urayama, K., Nagamatsu, Y., Takagahara, S., Turner, J. H., Kozasa, T., Kobayashi, H., Sato, Y., Kawanishi, T., Inoue, R., Nagao, T., and Kurose, H. (2005) *J. Biol. Chem.* **280,** 18434–18441
27. Fujii, T., Onohara, N., Maruyama, Y., Tanabe, S., Kobayashi, H., Fukutomi, M., Nagamatsu, Y., Nishihara, N., Inoue, R., Sumimoto, H., Shibasaki, F., Nagao, T., Nishida, M., and Kurose, H. (2005) *J. Biol. Chem.* **280,** 23041–23047
28. Pracyk, J. B., Tanaka, K., Hegland, D. D., Kim, K. S., Sethi, R., Rovira, I. I., Blazina, D. R., Lee, L., Bruder, J. T., Kovesdi, I., Goldshmidt-Clermont, P. J., Irani, K., and Finkel, T. (1998) *J. Clin. Invest.* **102,** 929–937
29. Sussman, M. A., Welch, S., Walker, A., Klevitsky, R., Hewett, T. E., Price, R. L., Schaefer, E., and Yager, K. (2000) *J. Clin. Invest.* **105,** 875–886
30. Ichiki, T., Takeda, K., Tokunou, T., Iino, N., Egashira, K., Shimokawa, H., Hirano, K., Kanaide, H., and Takeshita, A. (2001) *Arterioscler. Thromb. Vasc. Biol.* **21,** 1896–1901
31. Akira, S., Uematsu, S., and Takeuchi, O. (2006) *Cell* **124,** 783–801
32. Chao, W. (2009) *Am. J. Physiol. Heart Circ. Physiol.* **296,** H1–H12
33. Kurose, H., Arriza, J. L., and Lefkowitz, R. J. (1993) *Mol. Pharmacol.* **43,** 444–450
34. Nishida, M., Sato, Y., Uemura, A., Narita, Y., Tozaki-Saitoh, H., Nakaya, M., Ide, T., Suzuki, K., Inoue, K., Nagao, T., and Kurose, H. (2008) *EMBO J.* **27,** 3104–3115
35. Nishida, M., Sugimoto, K., Hara, Y., Mori, E., Morii, T., Kurosaki, T., and Mori, Y. (2003) *EMBO J.* **22,** 4677–4688
36. Nagamatsu, Y., Nishida, M., Onohara, N., Fukutomi, M., Maruyama, Y., Kobayashi, H., Sato, Y., and Kurose, H. (2006) *J. Pharmacol. Sci.* **101,** 144–150
37. Chiloeches, A., Paterson, H. F., Marais, R., Clerk, A., Marshall, C. J., and Sugden, P. H. (1999) *J. Biol. Chem.* **274,** 19762–19770
38. Franke, B., Akkerman, J. W., and Bos, J. L. (1997) *EMBO J.* **16,** 252–259
39. Arai, K., Maruyama, Y., Nishida, M., Tanabe, S., Takagahara, S., Kozasa, T., Mori, Y., Nagao, T., and Kurose, H. (2003) *Mol. Pharmacol.* **63,** 478–488
40. Ju, H., Zhao, S., Tappia, P. S., Panagia, V., and Dixon, I. M. (1998) *Circulation* **97,** 892–899
41. Bai, H., Wu, L. L., Xing, D. Q., Liu, J., and Zhao, Y. L. (2004) *Chin. Med. J.* **117,** 88–93
42. He, J., Gurunathan, S., Iwasaki, A., Ash-Shaheed, B., and Kelsall, B. L. (2000) *J. Exp. Med.* **191,** 1605–1610
43. Maruyama, Y., Nishida, M., Sugimoto, Y., Tanabe, S., Turner, J. H., Kozasa, T., Wada, T., Nagao, T., and Kurose, H. (2002) *Circ. Res.* **91,** 961–969
44. Nishida, M., Maruyama, Y., Tanaka, R., Kontani, K., Nagao, T., and Kurose, H. (2000) *Nature* **408,** 492–495

45. Cowling, R. T., Gurantz, D., Peng, J., Dillmann, W. H., and Greenberg, B. H. (2002) *J. Biol. Chem.* **277,** 5719–5724
46. Monks, B. G., Martell, B. A., Buras, J. A., and Fenton, M. J. (1994) *Mol. Immunol.* **31,** 139–151
47. Kaiser, P., Rothwell, L., Goodchild, M., and Bumstead, N. (2004) *Anim. Genet.* **35,** 169–175
48. Cowling, R. T., Zhang, X., Reese, V. C., Iwata, M., Gurantz, D., Dillmann, W. H., and Greenberg, B. H. (2005) *Am. J. Physiol. Heart Circ. Physiol.* **289,** H1176–H1183
49. Zocchi, M. R., Contini, P., Alfano, M., and Poggi, A. (2005) *J. Immunol.* **174,** 6054–6061
50. Ueyama, T., Eto, M., Kami, K., Tatsuno, T., Kobayashi, T., Shirai, Y., Lennartz, M. R., Takeya, R., Sumimoto, H., and Saito, N. (2005) *J. Immunol.* **175,** 2381–2390
51. van Hennik, P. B., ten Klooster, J. P., Halstead, J. R., Voermans, C., Anthony, E. C., Divecha, N., and Hordijk, P. L. (2003) *J. Biol. Chem.* **278,** 39166–39175
52. Brown, G. E., Stewart, M. Q., Liu, H., Ha, V. L., and Yaffe, M. B. (2003) *Mol. Cell* **11,** 35–47
53. Honbou, K., Minakami, R., Yuzawa, S., Takeya, R., Suzuki, N. N., Kamakura, S., Sumimoto, H., and Inagaki, F. (2007) *EMBO J.* **26,** 1176–1186
54. Gray, A., Van Der Kaay, J., and Downes, C. P. (1999) *Biochem. J.* **344,** 929–936
55. Rikitake, Y., and Liao, J. K. (2005) *Circ. Res.* **97,** 1232–1235
56. Ichiki, T., Takeda, K., Tokunou, T., Funakoshi, Y., Ito, K., Iino, N., and Takeshita, A. (2001) *Hypertension* **37,** 535–540
57. Laufs, U., Kilter, H., Konkol, C., Wassmann, S., Böhm, M., and Nickenig, G. (2002) *Cardiovasc. Res.* **53,** 911–920
58. Ito, M., Adachi, T., Pimentel, D. R., Ido, Y., and Colucci, W. S. (2004) *Circulation* **110,** 412–418
59. Bae, Y. S., Lee, J. H., Choi, S. H., Kim, S., Almazan, F., Witztum, J. L., and Miller, Y. I. (2009) *Circ. Res.* **104,** 210–218
60. Kamata, H., Honda, S., Maeda, S., Chang, L., Hirata, H., and Karin, M. (2005) *Cell* **120,** 649–661
61. Maack, C., Kartes, T., Kilter, H., Schäfers, H. J., Nickenig, G., Böhm, M., and Laufs, U. (2003) *Circulation* **108,** 1567–1574

European Journal of Pharmacology 635 (2010) 56–61

Contents lists available at ScienceDirect

European Journal of Pharmacology

journal homepage: www.elsevier.com/locate/ejphar

Neuropharmacology and Analgesia

Protective effect of all-trans retinoic acid on NMDA-induced neuronal cell death in rat retina

Kenji Sakamoto [a,*], Masahide Hiraiwa [a], Maki Saito [a], Tsutomu Nakahara [a], Yoji Sato [b], Taku Nagao [c], Kunio Ishii [a]

[a] Department of Molecular Pharmacology, Kitasato University School of Pharmaceutical Sciences, 9-1 Shirokane 5-chome, Minato-ku, Tokyo 108-8641, Japan
[b] Division of Cellular and Gene Therapy Products, National Institute of Health Sciences, 18-1 Kamiyoga 1-chome, Setagaya-ku, Tokyo 158-8501, Japan
[c] National Institute of Health Sciences, 18-1 Kamiyoga 1-chome, Setagaya-ku, Tokyo 158-8501, Japan

ARTICLE INFO

Article history:
Received 17 August 2009
Received in revised form 30 January 2010
Accepted 3 March 2010
Available online 19 March 2010

Keyword:
All-trans retinoic acid
Retina
N-methyl-D-aspartic acid
Extracellular signal-regulated kinase

ABSTRACT

We histologically examined the effects of all-trans retinoic acid (ATRA) on neuronal injury induced by intravitreous injection of N-methyl-D-aspartic acid (NMDA) (200 nmol/eye). Treatment with ATRA for 7 days (15 mg/kg for the first two days and 10 mg/kg for the following five days, p.o.) reduced the decrease of cell number in the ganglion cell layer and the inner nuclear layer 7 days after NMDA injection. TUNEL staining 6 h after NMDA injection showed that treatment with ATRA (15 mg/kg, p.o.) 1 h prior to NMDA injection reduced the number of apoptotic cells in the ganglion cell layer and inner nuclear layer. The anti-apoptotic effect of ATRA was vanished by intravitreous injection of U0126, an extracellular signal-regulated kinase/mitogen-activated protein kinase kinase inhibitor (1 nmol/eye). These results suggest that ATRA has a protective effect, which is medicated by extracellular signal-regulated kinase pathway, on NMDA-induced apoptosis in the rat retina. ATRA may be useful as a therapeutic drug against retinal diseases that cause glutamate neurotoxicity.

1. Introduction

Cell death of retinal ganglion cells is a characteristic of glaucoma, and the underlying mechanism is not completely understood. Stimulation of glutamate receptors by excess amount of glutamate under hypoxia (David et al., 1988) and ischemia–reperfusion (Louzada-Júnior et al., 1992) is toxic to neuronal cells. Activation of the N-methyl-D-aspartic acid (NMDA) receptor, a subtype of glutamate receptors (Choi, 1987, 1988), followed by excess Ca^{2+} influx *via* NMDA receptor-operated channels is involved in the predominant mechanism of neuronal excitotoxicity. In fact, excitotoxicity caused by the elevation of glutamate concentration in the retinal extracellular space near the glutamate receptors is thought to be one of the mechanisms of neuronal cell death induced by glaucoma (Kuehn et al., 2005).

Retinoids, including vitamin A and its derivatives, play important roles for regulating various biological processes, such as visual function, growth and differentiation (Chambon, 1996; Maden, 2001). Retinal and opsin comprise rhodopsin, which is very important for normal visual function (Palczewski et al., 2000). Retinoic acids regulate the expression of various genes by activation of their nuclear receptors, retinoic acid receptors and retinoid X receptors (Chambon, 1996; Maden, 2001). Retinoic acids bound to these receptors are transported to nucleus and work as transcription factors (Chambon, 1994). Recently, retinoic acids were reported to have rapid non-genomic effects on cytoplasmic messenger pathways. For example, retinoic acids have been reported to cause a rapid activation of extracellular signal-regulated kinase (ERK) through retinoic acid receptors and/or retinoid X receptors (Canon et al., 2004; Pasquali et al., 2005).

Retinoic acids are reported to play significant roles under pathological conditions. For instance, all-trans retinoic acid (ATRA) has a protective effect on oxygen–glucose deprivation-medicated cell death in the rat hippocampus slice *via* inhibition of c-jun N-terminal kinase and p38 mitogen-activated protein kinase (Shinozaki et al., 2007). Although retinoic acids have very important roles in the visual signal transduction, the role of the signaling cascade of retinoic acid in pathological conditions such as glaucoma in the retina still remains uncertain.

Mitogen-activated protein (MAP) kinase family plays important roles in the transduction of various extracellular stimuli to the nucleus. The family consists of three subgroups, extracellular signal-regulated kinase (ERK), c-jun N-terminal kinase (JNK) and p38 MAP kinase. Recent studies show that ATRA prevents neuronal cell death induced by beta-amyloid (Sahin et al., 2005), staurosporine (Ahlemeyer and Krieglstein, 1998), and oxygen–glucose deprivation (Shinozaki et al., 2007), and rapidly activated ERK *via* retinoic acid receptor in neuronal cells (Canon et al., 2004). Brain-derived neurotrophic factor and erythropoietin have been shown to protect against neuronal cell death induced by glutamate, hypoxia or ischemia *via* activation of ERK (Hetman et al., 1999; Han and Holtzman, 2000; Rössler et al., 2004; Kilic et al., 2005).

* Corresponding author. Tel./fax: +81 3 3444 6205.
E-mail address: sakamotok@pharm.kitasato-u.ac.jp (K. Sakamoto).

0014-2999/$ – see front matter © 2010 Elsevier B.V. All rights reserved.
doi:10.1016/j.ejphar.2010.03.001

Based on these finding shown above, we hypothesized that activation of retinoid acid signaling would protect against NMDA-induced neuronal cell death in the retina. In the present study, we demonstrated that ATRA protected the retinal neuron against apoptosis induced by NMDA. Because much better tolerance of retinoic acid was shown when using single doses (Teelmann, 1989), a single dose per day was chosen instead of multiple doses. The doses of ATRA used in this study were chosen according to doses tested in previous studies by other researchers. The dose of ATRA (15 mg/kg for the first two days and 10 mg/kg for the following five days, p.o.) has been shown to have anti-inflammatory properties in experimental rat models of nephropathy (Moreno-Manzano et al., 2003), to enhance nociceptive withdrawal reflexes in rats (Romero-Sandoval et al., 2004), and also to induce an increase in the prostaglandin E2 concentration in rat plasma and liver homogenate (Devaux et al., 2001). They were also well below the toxic doses reported in similar species (Teelmann, 1989). To test whether the protective effects of ATRA is dose-dependent, we tried one-third dose and three-time dose of ATRA. We also showed that the anti-apoptotic effect of ATRA was reduced by U0126, an extracellular signal-regulated kinase/mitogen-activated protein kinase kinase (MEK) inhibitor.

2. Materials and methods

2.1. Animals

In the present study, experimental procedures conformed to the Guiding Principles for the Care and Use of Laboratory Animals, approved by the Japanese Pharmacological Society. Male Sprague–Dawley rats weighing 230–300 g (Charles River Japan, Kanagawa, Japan) were used in the present study.

2.2. Intravitreous injection

Intravitreous injection was performed as previously described (Siliprandi et al., 1992; Sakamoto et al., 2009). Briefly, rats were anesthetized by intraperitoneal injection of sodium pentobarbital (50 mg/kg i.p.; Nembutal® injection, Abbott Laboratories, North Chicago, IL). Injection was performed with a 33-gauge needle connected to a 25-μl gas-tight microsyringe (1702LT, Hamilton, Reno, NV). The tip of the needle was inserted approximately 1 mm behind the corneal limbus. Five μl of the drug solution described below was administered into one eye and vehicle was administered into another eye as control.

2.3. Preparation of drugs

NMDA (Nacalai Tesque, Kyoto, Japan) were dissolved in saline. All-trans retinoic acid (ATRA) (Sigma, St. Louis, MO) was suspended in 0.5% carboxymethyl cellulose (CMC) (Nacalai Tesque), and orally administered. The final volume of the suspension is 0.5 ml. A similar amount of 0.5% CMC was administered to the control animals. In the continuous administration with either ATRA or vehicle for seven days, the dose of ATRA in the first two days was 5, 15 or 45 mg/kg and the dose in the following five days was 3, 10 or 30 mg/kg, respectively. In the single administration of ATRA, 15 mg/kg ATRA was treated. The first dose of ATRA or the vehicle was administered orally 1 h before NMDA injection. We prepared 0.4 M stock solutions of U0126 (Promega, Madison, WI) and diluted it to working concentration (2×10^{-4} M or 4×10^{-4} M) with saline. U0126 or the vehicle was administrated intravitreously 15 min before treatment of ATRA.

2.4. Histological evaluation

The method for histological evaluation was described previously (Sakamoto et al., 2006; Sakamoto et al., 2009). The method is a modification of the one employed by some other groups (LaVail and Battelle, 1975; Unoki and LaVail, 1994; Roth et al., 1998; Toriu et al., 2000). Animals were euthanized by overdosage of pentobarbital sodium 7 days after intravitreous NMDA injection and both eyes were enucleated. Enucleated eyes were fixed with Davidson solution, comprised of 37.5% ethanol, 9.3% paraformaldehyde, 12.5% acetic acid and 3% glutaraldehyde for 1–12 h at room temperature. The fixed eye was bisected through the optic nerve head in the vertical meridian with a microtome blade (Histo Cutter Super #35 Type, Micro Glass, Tokyo, Japan) and embedded in paraffin after removing a lens. Five μm horizontal sections through the optic nerve head of the eye were cut along the vertical meridian of the eye so as to contain the entire retina from the ora serrata in the superior hemisphere to the ora serrata in the inferior hemisphere using a microtome (HM325, Microm International, Walldorf, Germany) and a microtome blade (Histo Cutter Super #35 Type, Micro Glass). The sections were stained with hematoxylin and eosin, and subject to morphometry. The sections which showed oblique regions were excluded to avoid artifacts. The total number of the cells in the retinal ganglion cell layer (GCL) was counted for a length of 1 mm on either side of the optic nerve head beginning approximately 1 mm from the center of the optic nerve head in four independent sections using a light microscope (Optiphot-2, Nicon, Tokyo, Japan). No attempt was made to distinguish the cell types in the GCL, and displaced amacrine cells were not excluded from the counts. Measurement of the thickness of the inner plexiform layer (IPL), the inner nuclear layer (INL) and the outer nuclear layer (ONL) was also performed to quantify the degree of cell loss induced by intravitreous NMDA injection. Digital photographs with approximately 0.25 mm width of the retinal layers in each section at a distance of approximately 1 mm from the center of the optic nerve head were taken using a digital camera (DP11, Olympus, Tokyo, Japan) connected to a light microscope. The photographs were printed onto A4 papers. Lines indicating the inner and outer borders of INL and ONL and the bottom of the ganglion cells were drawn on the printed photographs. To know the thicknesses of IPL, INL and ONL, the distance between the lines on the paper was measured. The areas which measured the distance were spaced at approximately 40 μm intervals. Averages for these measurements of thickness taken in five adjacent areas were calculated. These parameters of each eye injected NMDA were normalized with those of the corresponding intact opposite eyes and are presented as percentages. We did all of the morphometrical analysis in a blind fashion.

2.5. Deoxy UTP-biotin nick-end labeling assay

The method for terminal deoxynucleotidyl transferase-mediated dUTP-biotin nick-end labeling (TUNEL) assay was described previously (Sakamoto et al., 2009). To examine whether ATRA inhibits apoptosis induced by intravitreous NMDA injection, TUNEL assay was performed. Intravitreous NMDA injection was performed as described above in one eye and saline was injected to another eye as control. Animals were euthanized by overdosage of pentobarbital sodium 6 h after NMDA injection and both eyes were enucleated. Enucleated eyes were fixed with Davidson solution described above for 1 h at room temperature. Fixed retinal tissues were cryoprotected in Holt's hypertonic gum sucrose solution, comprised of 0.1% thymol, 1% gum acacia and 30% sucrose in distilled water, overnight at 4 °C. Ten-μm-thick sections of retina through the optic disk were then cut with a cryostat (HM 500, Microm International, Walldorf, Germany). The TUNEL assay was performed with ApoTag peroxidase in situ apoptosis detection kit (Chemicon, Temecula, CA), according to the manufacturer's instructions. For nuclear staining, the specimens were counterstained with methylgreen (Wako Pure Chemical, Osaka, Japan). We counted the number of TUNEL-positive nuclei in GCL and INL for a length of 1 mm on either side of the optic nerve head

beginning approximately 1 mm from the center of the optic nerve head manually using a light microscope.

2.6. Statistical analysis

The data represent the means ± S.E.M. of three to ten rats per group. One way analysis of variance followed by Tukey–Kramer test was used for multiple comparisons. Differences were considered to be statistically significant when the P values were less than 0.05.

3. Results

3.1. Effect of ATRA on the retinal injury induced by the intravitreous NMDA injection

At first, we determined the effects of ATRA on the retinal injury induced by intravitreous NMDA injection. Typical photomicrographs of the retina taken 7 days after NMDA injection are shown in Fig. 1. In the vehicle-treated group, degenerative changes were observed in GCL and IPL of the NMDA-injected eye, a characteristic of retinal atrophy (Fig. 1B), but such changes were not seen in the contralateral control retina (Fig. 1A). Morphometric results at 7 days after NMDA injection of three to 10 independent experiments are shown in Fig. 2. As indicated by the morphologic analysis, the IPL in the NMDA-injected eye was thinner than in the contralateral saline-injected eye at 7 days after injection. No significant change was seen in the thickness of OPL and ONL after injection in all of the groups. Treatment with 15 mg/kg (the first two days) and 10 mg/kg (the following five days) (Fig. 1D), but not 5 mg/kg (the first two days) and 3 mg/kg (the following five days) (Fig. 1C), ATRA 60 min before NMDA injection significantly reduced the amount of retinal damage.

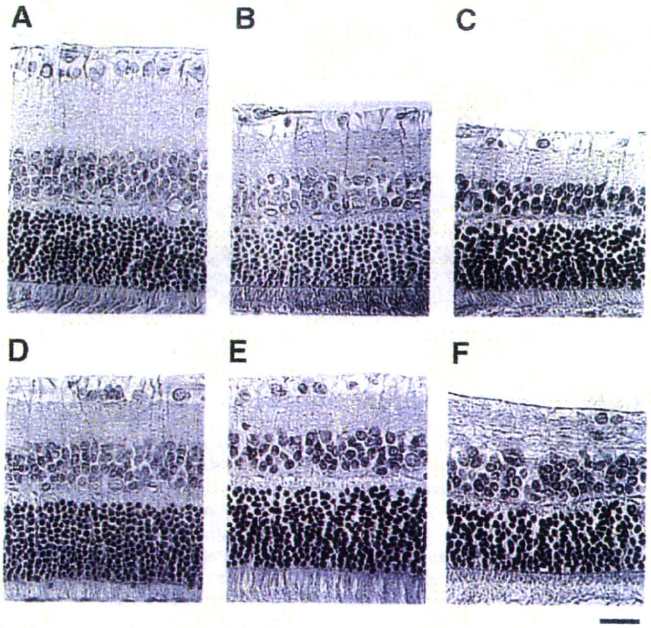

Fig. 1. Representative photomicrographs showing histological appearance of the vehicle-injected control (A), and NMDA-injected retinae 7 days after NMDA injection (B, C and D). ATRA was orally treated 60 min before NMDA injection. Retinal damage is shown in CMC (the vehicle of ATRA)-treated ($n = 10$) (B), 5 mg/kg (the first two days) and 3 mg/kg (the following five days) ATRA-treated ($n = 3$) (C) retinae. In the 15 mg/kg (the first two days) and 10 mg/kg (the following five days) ATRA-treated group, retinal structure is preserved ($n = 8$) (D). The results of 45 mg/kg (the first two days) and 30 mg/kg (the following five days) ATRA-treated group could be divided into the two groups ($n = 4$). Similar protective effects to those in the 15 mg/kg (the first two days) and 10 mg/kg (the following five days) ATRA-treated group was seen in 2 out of 4 animals (E), whereas no protection could be seen in others (F). Scale bar = 50 μm. Original magnification is ×200.

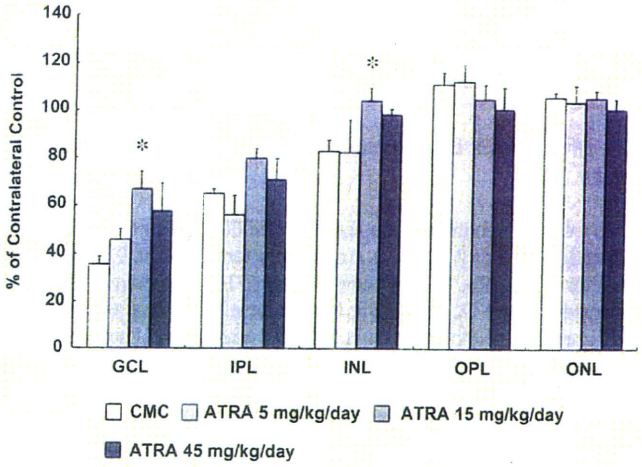

Fig. 2. Effect of ATRA treated orally on the histological damage induced by intravitreously NMDA injection. Retinal damage was examined 7 days after NMDA injection. The following 4 parameters of the NMDA-injected eyes were normalized to those of the vehicle-injected eyes (the opposite side of the NMDA-injected eye) and are presented as percentages: cell density in the GCL (ganglion cell layer) and the INL (inner nuclear layer); thickness of the IPL (inner plexiform layer), OPL (outer plexiform layer) and the ONL (outer nuclear layer). The data represent the means ± S.E.M. of three to ten rats per group. *$P < 0.05$, vs. CMC-treated group.

The results of 45 mg/kg (the first two days) and 30 mg/kg (the following five days) ATRA-treated group could be divided into two groups. Similar protective effects to those in the 15 mg/kg (the first two days) and 10 mg/kg (the following five days) ATRA-treated group were seen in 2 out of 4 animals (Fig. 1E), whereas no protection could be seen in others (Fig. 1F). These results indicated that 15 mg/kg (the first two days) and 10 mg/kg (the following five days) ATRA is the best dose to protect against the NMDA-induced retinal damage. Oral treatment with ATRA itself did not affect the retinal morphology.

3.2. Effect of ATRA on apoptosis induced by the intravitreous NMDA injection in the rat retina

To examine whether ATRA reduces apoptotic cell death induced by intravitreous NMDA injection, we conducted TUNEL staining of the retina 6 h after NMDA injection. As shown in Fig. 3, TUNEL-positive cells were observed in the GCL and in the inner side of the INL, but not in the ONL, in the vehicle-treated group. Oral treatment with ATRA at

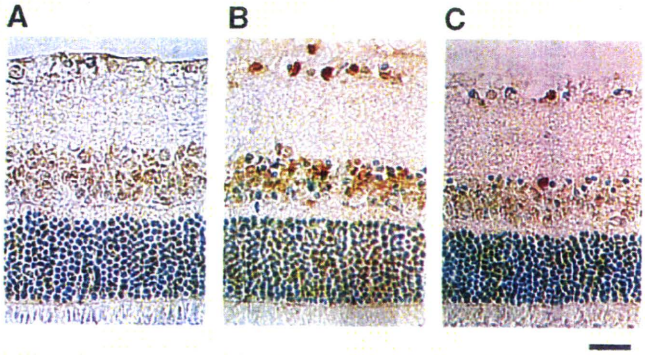

Fig. 3. Representative photomicrographs showing TUNEL staining of the vehicle-injected control and NMDA-injected retinae 6 h after NMDA injection. TUNEL-positive nuclei are shown in ganglion cell layer and inner nuclear layer of CMC (the vehicle of ATRA)-treated and NMDA-injected retinae ($n = 4$) (B), whereas no TUNEL-positive cell was seen in CMC-treated and the vehicle of NMDA-injected retinae (the opposite side of the NMDA-injected eye) (A). In the retina treated with 15 mg/kg ATRA 60 min before NMDA injection, the number of the positive nuclei in the ganglion cell layer and the inner nuclear layer is smaller than that in the CMC and NMDA-treated retinae ($n = 4$) (C). Scale bar = 50 μm. Original magnification is ×200.

15 mg/kg 60 min before NMDA injection markedly reduced TUNEL-positive cells. Results of cell count in GCL and INL of three to four independent experiments are shown in Fig. 4.

3.3. Effect of MEK inhibitor on anti-apoptotic effect of ATRA in the rat retina

To examine whether the activation of ERK is involved in the anti-apoptotic effect of ATRA, we co-administrated with U0126, a MEK inhibitor and ATRA. As shown in Fig. 5, TUNEL-positive cells were observed in the GCL and in the inner side of the INL, but not in the ONL, in the retina of the animals treated both U0126 (1 nmol, 15 min before ATRA treatment) and ATRA (15 mg/kg, 60 min before NMDA injection). U0126 (1 nmol) itself did not affect the apoptosis induced by intravitreous NMDA injection. U0126 (2 nmol) itself reduced the number of TUNEL-positive cells in GCL, whereas the concentration of U0126 tended to block the protective effects of ATRA in INL. Results of cell count in GCL and INL of three to four independent experiments are shown in Fig. 6.

4. Discussion

In the present study, we demonstrated that ATRA has a protective effect on NMDA-induced neuron damage and an anti-apoptotic effect in the rat retina *in vivo*. The dose of ATRA which showed the protective effects in the present study (15 mg/kg for the first two days and 10 mg/kg for the following five days) has been shown to have anti-inflammatory properties in an experimental rat models of nephropathy (Moreno-Manzano et al., 2003), to enhance nociceptive withdrawal reflexes in rats (Romero-Sandoval et al., 2004), and also to induce an increase in the prostaglandin E2 concentration in rat plasma and liver homogenate (Devaux et al., 2001), and the doses were also well below the toxic doses reported in the similar species (Teelmann, 1989). In addition, no protective effect was seen in some animals treated with the highest dose of ATRA in the present study. Although the reason why the highest dose did not induce protective effects could not be clarified in the present study, it is possible that some pro-apoptotic signals may be activated simultaneously by the dose of ATRA. Because the dose of ATRA itself did not affect retinal morphology, toxicity of ATRA is much less likely to be involved in the underlying mechanism. We propose that the middle dose of ATRA in the present study (15 mg/kg for the first two days and 10 mg/kg for the following five days) is the best to bring its beneficial effects in our experimental model and maybe also in other experimental models using the rats.

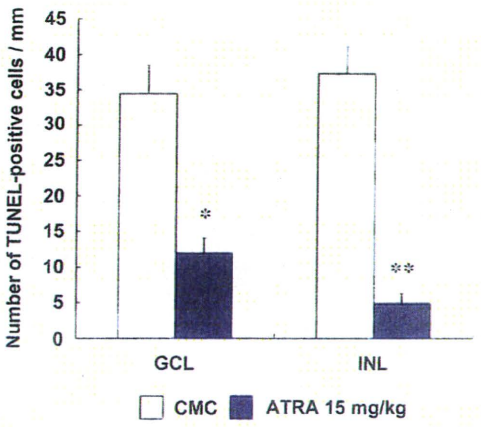

Fig. 4. The result of TUNEL-positive cell count. TUNEL staining was examined 6 h after NMDA injection. The number of TUNEL-positive cells was counted manually at 1.0 mm from the center of the optic disk using a microscope: GCL (ganglion cell layer); INL (inner nuclear layer). The data represent the means ± S.E.M. of four rats per group. *P< 0.05, **P< 0.01 vs. CMC-treated group.

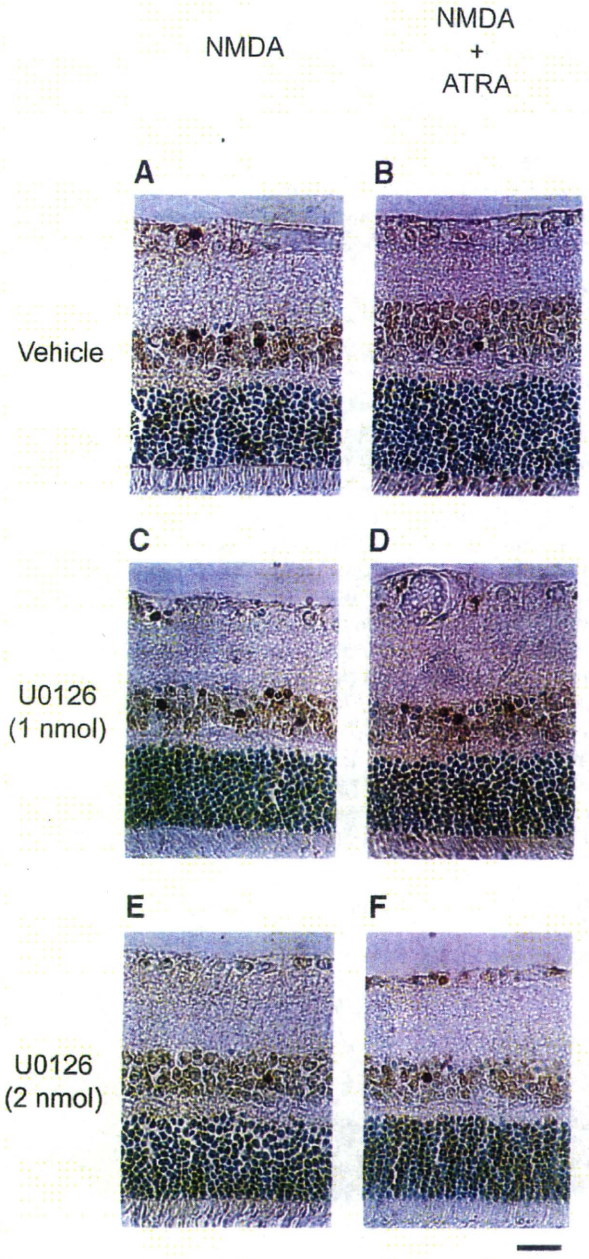

Fig. 5. Representative photomicrographs showing the effect of U0126, an extracellular signal-regulated kinase/mitogen-activated protein kinase kinase (MEK) inhibitor, on anti-apoptotic action of ATRA. TUNEL-positive nuclei are shown in the ganglion cell layer and the inner nuclear layer of CMC (the vehicle of ATRA)-treated and NMDA and the vehicle of U0126-injected retinae ($n=5$) (A). In the retina treated with 15 mg/kg ATRA 60 min before NMDA and the vehicle of U0126 injection, the number of the positive nuclei is smaller than that in the CMC and NMDA-treated retinae ($n=3$) (B). TUNEL-positive nuclei are shown in the ganglion cell layer and the inner nuclear layer of CMC-treated and the vehicle of NMDA and U0126-injected retinae ($n=5$) (C). In the retina treated with 15 mg/kg ATRA 60 min before NMDA and 1 nmol/eye U0126 injection, the number of the positive nuclei is larger than that in the ATRA and NMDA-treated retinae ($n=5$) (D). In the retina injected 2 nmol/eye U0126 injection, the numbers of TUNEL-positive cells were reduced with (F; $n=6$) or without (E; $n=3$) treatment with ATRA. Scale bar = 50 μm. Original magnification is ×200.

Retinoic acid has not only genomic effects, such as induction of various genes, but also rapid non-genomic effects on cytoplasmic messenger pathways. In the present study, we found that oral administration of ATRA 60 min before NMDA injection led to the

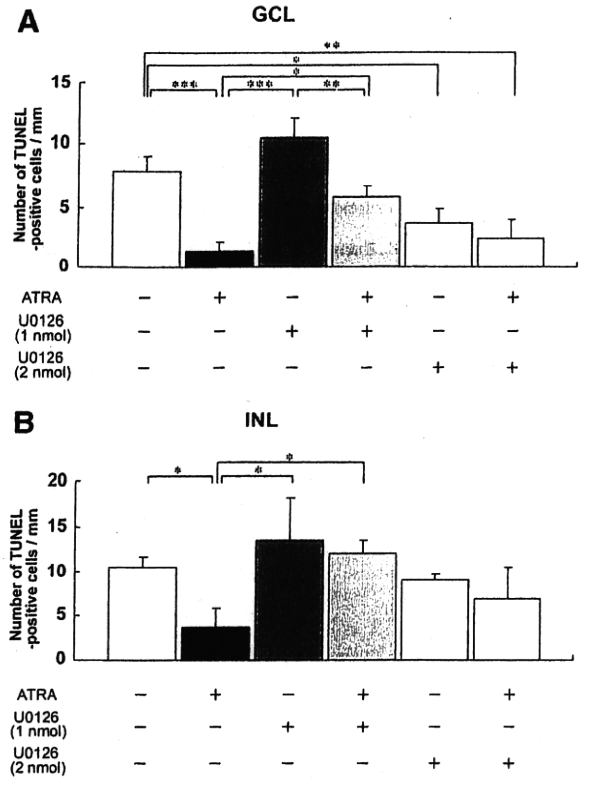

Fig. 6. The result of TUNEL-positive cell count in the experiments using U0126. TUNEL staining was examined 6 h after NMDA injection. The number of TUNEL-positive cells was counted manually at 1.0 mm from the center of the optic disk using a microscope: GCL (ganglion cell layer); INL (inner nuclear layer). The data represent the means ± S.E.M. of three to five rats per group. $^{*}P<0.05$, $^{**}P<0.01$, $^{***}P<0.001$ between the indicated groups.

neuroprotection in retina. The anti-apoptotic effect of ATRA is unlikely to be mediated by the genomic action of its nuclear receptors, because it usually takes at least a few hours. In addition, the anti-apoptotic effect was inhibited by 1 nmol/eye U0126, a MEK inhibitor. Because 2 nmol/eye U0126 itself reduced apoptosis induced by NMDA in GCL, it is possible that the dose of U0126 nonselectively inhibited pro-apoptotic kinases, such as JNK and p38 MAP kinase in GCL. The results in the present study also suggest that 1 nmol/eye is the best dose to block ERK in our experimental system. To strengthen the involvement of MEK in ATRA-induced protection, we tried to see the effects of U0126 on the histological protection by ATRA 7 days after NMDA injection, and the effects of PD098059, another MEK inhibitor. Unfortunately, we gave these experiments up, because of the damage of eyeballs induced by repetitive intravitreous injection, and anti-apoptotic effects of its vehicle, respectively. ATRA is known to activate neuronal ERK through retinoic acid receptors and/or retinoid X receptors in a non-genomic manner (Canon et al., 2004). ATRA has also been shown to inhibit the dephosphorylation of ERK in the oxygen–glucose-deprived rat cultured hippocampus slice (Shinozaki et al., 2007). To combine our results and previous reports, it is possible that ATRA activates ERK *via* its non-genomic action, leading to the protection of retinal neurons from NMDA-induced apoptosis.

ATRA is known to induce the expression of mitogen-activated protein kinase phosphatase-1 (MKP-1), which protects mesangial cells against hydrogen peroxide-induced cell death by dephosphorylation of JNK and p38 MAP kinase (Konta et al., 2001). MKP-1 has been reported to dephosphorylate JNK and p38 MAP kinase, but not ERK (Wu and Bennett, 2005). In the previous study, ATRA has been shown to inhibit the activation of JNK and p38 MAP kinase, which are pro-apoptotic signals in the oxygen–glucose-deprived rat cultured hippocampus slice (Shinozaki et al., 2007). Therefore, it is of interest to examine whether the inhibition of JNK and p38 by ATRA also plays a significant role in its cytoprotective effect in the retina. To clarify this point, further progress of the reagents that selectively activate JNK and/or p38 MAP kinase, and experiments using such reagents are needed.

In conclusion, the present study indicates that ATRA has a protective effect on retinal neurons against NMDA-induced apoptosis *in vivo*. The activation of ERK is possible to be involved in the underlying mechanisms. ATRA easily passes through the blood–brain barrier and reach the central nervous system (Crandall et al., 2004). Because of its lipophilic nature, orally administered ATRA presumably passes through the blood-retinal barrier relatively easily. Our findings suggest that ATRA may be effective for treatment of retinal diseases known to be associated with glutamate excitotoxicity such as retinal vessel occlusion and glaucoma.

Acknowledgments

This work is supported by the Japanese Ministry of Education, Science, Sports and Culture, Grant-in-Aid for Young Scientists (B) #17790174 (KS), and grants from the Japanese Ministry of Health, Labor and Welfare and the Japan Health Sciences Foundation #KHC1014 (YS).

References

Ahlemeyer, B., Krieglstein, J., 1998. Retinoic acid reduces staurosporine-induced apoptotic damage in chick embryonic neurons by suppressing reactive oxygen species production. Neurosci. Lett. 246, 93–96.
Canon, E., Cosgaya, J.M., Scsucova, S., Aranda, A., 2004. Rapid effects of retinoic acid on CREB and ERK phosphorylation in neuronal cells. Mol. Biol. Cell 15, 5583–5592.
Chambon, P., 1994. The retinoid signaling pathway: molecular and genetic analyses. Semin. Cell Biol. 5, 115–125.
Chambon, P., 1996. A decade of molecular biology of retinoic acid receptors. FASEB J. 10, 940–954.
Choi, D.W., 1987. Ionic dependence of glutamate neurotoxicity in cortical cell culture. J. Neurosci. 7, 369–379.
Choi, D.W., 1988. Calcium-mediated neurotoxicity: relationship to specific channel types and role in ischemic damage. Trends Neurosci. 11, 465–469.
Crandall, J., Sakai, Y., Zhang, J., Koul, O., Mineur, Y., Crusio, W.E., McCaffery, P., 2004. 13-Cis-retinoic acid suppresses hippocampal cell division and hippocampal-dependent learning in mice. Proc. Natl. Acad. Sci. U. S. A. 101, 5111–5116.
David, P., Lusky, M., Teichberg, V.I., 1988. Involvement of excitatory neurotransmitters in the damage produced in chick embryo retinas by anoxia and extracellular high potassium. Exp. Eye Res. 46, 657–662.
Devaux, Y., Seguin, C., Grosjean, S., de Talancé, N., Schwartz, M., Burlet, A., Zannad, F., Meistelman, C., Mertes, P.M., Ungureanu-Longrois, D., 2001. Retinoic acid and lipopolysaccharide act synergistically to increase prostanoid concentrations in rats in vivo. J. Nutr. 131, 2628–2635.
Han, B.H., Holtzman, D.M., 2000. BDNF protects the neonatal brain from hypoxic–ischemic injury in vivo via the ERK pathway. J. Neurosci. 20, 5775–5781.
Hetman, M., Kanning, K., Cavanaugh, J.E., Xia, Z., 1999. Neuroprotection by brain-derived neurotrophic factor is mediated by extracellular signal-regulated kinase and phosphatidylinositol 3-kinase. J. Biol. Chem. 274, 22569–22580.
Kilic, E., Kilic, U., Soliz, J., Bassetti, C.L., Gassmann, M., Hermann, D.M., 2005. Brain-derived erythropoietin protects from focal cerebral ischemia by dual activation of ERK-1/-2 and Akt pathways. FASEB J. 19, 2026–2028.
Konta, T., Xu, Q., Furusu, A., Nakayama, K., Kitamura, M., 2001. Selective roles of retinoic acid receptor and retinoid x receptor in the suppression of apoptosis by all-trans-retinoic acid. J. Biol. Chem. 276, 12697–12701.
Kuehn, M.H., Fingert, J.H., Kwon, Y.H., 2005. Retinal ganglion cell death in glaucoma: mechanisms and neuroprotective strategies. Ophthalmol. Clin. North Am. 18, 383–395.
LaVail, M.M., Battelle, B.A., 1975. Influence of eye pigmentation and light deprivation on inherited retinal dystrophy in the rat. Exp. Eye Res. 21, 167–192.
Louzada-Júnior, P., Dias, J.J., Santos, W.F., Lachat, J.J., Bradford, H.F., Coutinho-Netto, J., 1992. Glutamate release in experimental ischaemia of the retina: an approach using microdialysis. J. Neurochem. 59, 358–363.
Maden, M., 2001. Role and distribution of retinoic acid during CNS development. Int. Rev. Cytol. 209, 1–77.
Moreno-Manzano, V., Mampaso, F., Sepúlveda-Muñoz, J.C., Alique, M., Chen, S., Ziyadeh, F.N., Iglesias-de la Cruz, M.C., Rodríguez, J., Nieto, E., Orellana, J.M., Reyes, P., Arribas, I., Xu, Q., Kitamura, M., Lucio Cazana, F.J., 2003. Retinoids as a potential treatment for experimental puromycin-induced nephrosis. Br. J. Pharmacol. 139, 823–831.
Palczewski, K., Kumasaka, T., Hori, T., Behnke, C.A., Motoshima, H., Fox, B.A., Le Trong, I., Teller, D.C., Okada, T., Stenkamp, R.E., Yamamoto, M., Miyano, M., 2000. Crystal structure of rhodopsin: a G protein-coupled receptor. Science 289, 739–745.
Pasquali, D., Chieffi, P., Deery, W.J., Nicoletti, G., Bellastella, A., Sinisi, A.A., 2005. Differential effects of all-trans-retinoic acid (RA) on Erk1/2 phosphorylation and

cAMP accumulation in normal and malignant human prostate epithelial cells: Erk1/2 inhibition restores RA-induced decrease of cell growth in malignant prostate cells. Eur. J. Endocrinol. 152, 663–669.

Romero-Sandoval, E.A., Alique, M., Moreno-Manzano, V., Molina, C., Lucio, F.J., Herrero, J.F., 2004. The oral administration of retinoic acid enhances nociceptive withdrawal reflexes in rats with soft-tissue inflammation. Inflamm. Res. 53, 297–303.

Rössler, O.G., Giehl, K.M., Thiel, G., 2004. Neuroprotection of immortalized hippocampal neurons by brain-derived neurotrophic factor and Raf-1 protein kinase: role of extracellular signal-regulated protein kinase and phosphatidylinositol 3-kinase. J. Neurochem. 88, 1240–1252.

Roth, S., Li, B., Rosenbaum, P.S., Gupta, H., Goldstein, I.M., Maxwell, K.M., Gidday, J.M., 1998. Preconditioning provides complete protection against retinal ischemic injury in rats. Invest. Ophthalmol. Vis. Sci. 39, 777–785.

Sahin, M., Karauzum, S.B., Perry, G., Smith, M.A., Aliciguzel, Y., 2005. Retinoic acid isomers protect hippocampal neurons from amyloidbeta induced neurodegeneration. Neurotox. Res. 7, 243–250.

Sakamoto, K., Yonoki, Y., Kubota, Y., Kuwagata, M., Saito, M., Nakahara, T., Ishii, K., 2006. Inducible nitric oxide synthase inhibitors abolished histological protection by late ischemic preconditioning in rat retina. Exp. Eye Res. 82, 512–518.

Sakamoto, K., Kawakami, T., Shimada, M., Yamaguchi, A., Kuwagata, M., Saito, M., Nakahara, T., Ishii, K., 2009. Histological protection by cilnidipine, a dual L/N-type Ca^{2+} channel blocker, against neurotoxicity induced by ischemia–reperfusion in rat retina. Exp. Eye Res. 88, 974–982.

Shinozaki, Y., Sato, Y., Koizumi, S., Ohno, Y., Nagao, T., Inoue, K., 2007. Retinoic acids acting through retinoid receptors protect hippocampal neurons from oxygen-glucose deprivation-mediated cell death by inhibition of c-jun-N-terminal kinase and p38 mitogen-activated protein kinase. Neuroscience 147, 153–163.

Siliprandi, R., Canella, R., Carmignoto, G., Schiavo, N., Zanellato, A., Zanoni, R., Vantini, G., 1992. N-methyl-D-aspartate-induced neurotoxicity in the adult rat retina. Vis. Neurosci. 8, 567–573.

Teelmann, K., 1989. Retinoids: toxicology and teratogenicity to date. Pharmacol. Ther. 40, 29–43.

Toriu, N., Akaike, A., Yasuyoshi, H., Zhang, S., Kashii, S., Honda, Y., Shimazawa, M., Hara, H., 2000. Lomerizine, a Ca^{2+} channel blocker, reduces glutamate-induced neurotoxicity and ischemia/reperfusion damage in rat retina. Exp. Eye Res. 70, 475–484.

Unoki, K., LaVail, M.M., 1994. Protection of the rat retina from ischemic injury by brain-derived neurotrophic factor, ciliary neurotrophic factor, and basic fibroblast growth factor. Invest. Ophthalmol. Vis. Sci. 35, 907–915.

Wu, J.J., Bennett, A.M., 2005. Essential role for mitogen-activated protein (MAP) kinase phosphatase-1 in stress-responsive MAP kinase and cell survival signaling. J. Biol. Chem. 280, 16461–16466.

THE JOURNAL OF BIOLOGICAL CHEMISTRY VOL. 285, NO. 17, pp. 13244–13253, April 23, 2010

Phosphorylation of TRPC6 Channels at Thr^{69} Is Required for Anti-hypertrophic Effects of Phosphodiesterase 5 Inhibition*

Received for publication, October 8, 2009, and in revised form, February 12, 2010 Published, JBC Papers in Press, February 22, 2010, DOI 10.1074/jbc.M109.074104

Motohiro Nishida[‡], Kenta Watanabe[‡], Yoji Sato[§], Michio Nakaya[‡], Naoyuki Kitajima[‡], Tomomi Ide[¶], Ryuji Inoue[‖], and Hitoshi Kurose[‡1]

From the [‡]Department of Pharmacology and Toxicology, Graduate School of Pharmaceutical Sciences, and the [¶]Department of Cardiovascular Medicine, Graduate School of Medical Sciences, Kyushu University, Higashi-ku, Fukuoka 812-8582, the [§]Division of Cellular and Gene Therapy Products, National Institute of Health Sciences, Setagaya, Tokyo 158-8501, and the [‖]Department of Physiology, School of Medicine, Fukuoka University, 7-45-1 Nanakuma, Jyonan-ku, Fukuoka 814-0180, Japan

Activation of Ca^{2+} signaling induced by receptor stimulation and mechanical stress plays a critical role in the development of cardiac hypertrophy. A canonical transient receptor potential protein subfamily member, TRPC6, which is activated by diacylglycerol and mechanical stretch, works as an upstream regulator of the Ca^{2+} signaling pathway. Although activation of protein kinase G (PKG) inhibits TRPC6 channel activity and cardiac hypertrophy, respectively, it is unclear whether PKG suppresses cardiac hypertrophy through inhibition of TRPC6. Here, we show that inhibition of cGMP-selective PDE5 (phosphodiesterase 5) suppresses endothelin-1-, diacylglycerol analog-, and mechanical stretch-induced hypertrophy through inhibition of Ca^{2+} influx in rat neonatal cardiomyocytes. Inhibition of PDE5 suppressed the increase in frequency of Ca^{2+} spikes induced by agonists or mechanical stretch. However, PDE5 inhibition did not suppress the hypertrophic responses induced by high KCl or the activation of protein kinase C, suggesting that PDE5 inhibition suppresses Ca^{2+} influx itself or molecule(s) upstream of Ca^{2+} influx. PKG activated by PDE5 inhibition phosphorylated TRPC6 proteins at Thr^{69} and prevented TRPC6-mediated Ca^{2+} influx. Substitution of Ala for Thr^{69} in TRPC6 abolished the anti-hypertrophic effects of PDE5 inhibition. In addition, chronic PDE5 inhibition by oral sildenafil treatment actually induced TRPC6 phosphorylation in mouse hearts. Knockdown of RGS2 (regulator of G protein signaling 2) and RGS4, both of which are activated by PKG to reduce $G\alpha_q$-mediated signaling, did not affect the suppression of receptor-activated Ca^{2+} influx by PDE5 inhibition. These results suggest that phosphorylation and functional suppression of TRPC6 underlie prevention of pathological hypertrophy by PDE5 inhibition.

Pathological hypertrophy of the heart, induced by pressure overload, such as chronic hypertension and aortic stenosis, is a major risk factor for heart failure and cardiovascular mortality (1). Neurohumoral factors, such as norepinephrine, angiotensin II (Ang II),[2] and endothelin-1 (ET-1), and mechanical stress are believed to be prominent contributors for pressure overload-induced cardiac hypertrophy (2, 3). Neurohumoral factors stimulate G_q protein-coupled receptors, leading to a sustained increase in $[Ca^{2+}]_i$ through activation of phospholipase C. Mechanical stress also increases $[Ca^{2+}]_i$ through Ca^{2+} influx-dependent pathways (4). The increase in $[Ca^{2+}]_i$ induces activation of Ca^{2+}-sensitive effectors, such as Ca^{2+}/calmodulin-dependent serine/threonine phosphatase calcineurin (3, 5), Ca^{2+}/calmodulin-dependent kinase II (6, 7), and calmodulin-binding transcription factor (8), which in turn induces hypertrophic gene expressions. Although the mechanism of Ca^{2+}-mediated hypertrophy is extensively analyzed, it is not fully understood how these Ca^{2+} targets specifically decode the alteration of $[Ca^{2+}]_i$ under the conditions of the rhythmic Ca^{2+} increases required for contraction.

In excitable cardiomyocytes, increases in the frequency or amplitude of Ca^{2+} transients evoked by Ca^{2+} influx-induced Ca^{2+} release have been suggested to encode signals for induction of hypertrophy (9). A partial depolarization of plasma membrane by receptor stimulation is reported to increase the frequency of Ca^{2+} oscillations, leading to activation of nuclear factor of activated T cells (NFAT), a transcription factor that is predominantly regulated by calcineurin (10). Recent reports have indicated that transient receptor potential canonical (TRPC) subfamily proteins play an essential role in agonist-induced membrane depolarization (11, 12). The relevance of TRPC channels to pathological hypertrophy is underscored by the observations that heart-targeted transgenic mice expressing TRPC channels caused hypertrophy (13, 14) and that TRPC proteins were up-regulated in hypertrophied and failing hearts (14–17). Among seven TRPC subfamilies, increased channel activities of TRPC1, TRPC3, and TRPC6 have been implicated in cardiac hypertrophy *in vivo*. TRPC1 is known to function not

* This study was supported by grants from the Ministry of Education, Culture, Sports, Science, and Technology of Japan (to M. Nishida, M. Nakaya, and H. Kurose), a grant-in-aid for scientific research on Innovative Areas (to M. Nishida), a grant-in-aid for scientific research on Priority Areas (H. Kurose), and grants from the Naito Foundation, the Nakatomi Foundation, the Sapporo Bioscience Foundation (M. Nishida), and the Mochida Memorial Foundation for Medical and Pharmaceutical Research (to M. Nakaya).

[1] To whom correspondence should be addressed. Tel./Fax: 81-92-642-6884; E-mail: kurose@phar.kyushu-u.ac.jp.

[2] The abbreviations used are: Ang II, angiotensin II; BNP, brain natriuretic peptide; CA-NFAT, constitutively active NFAT; DAG, diacylglycerol; $DiBAC_4(3)$, bis(1,3-dibutylbarbituric acid)trimethine oxonol; DN-TRPC6, dominant negative TRPC6; ET-1, endothelin-1; BTP2, 4-methyl-4′-[3,5-bis(trifluoromethyl)-1H-pyrazol-1-yl]-1,2,3-thiadiazole-5-carboxanilide; NFAT, nuclear factor of activated T cells; OAG, a DAG derivative, 1-oleoyl-2-acetyl-*sn*-glycerol; TRPC, transient receptor potential canonical; PDE5-I, phosphodiesterase 5-selective inhibitor: 4-{[3′,4′-(methylenedioxy)benzyl]amino}-6-methoxyquinazoline; RGS, regulator of G protein signaling; PKG, protein kinase G; WT, wild type; 8-Br-cGMP, 8-bromo-cyclic GMP; siRNA, small interfering RNA.

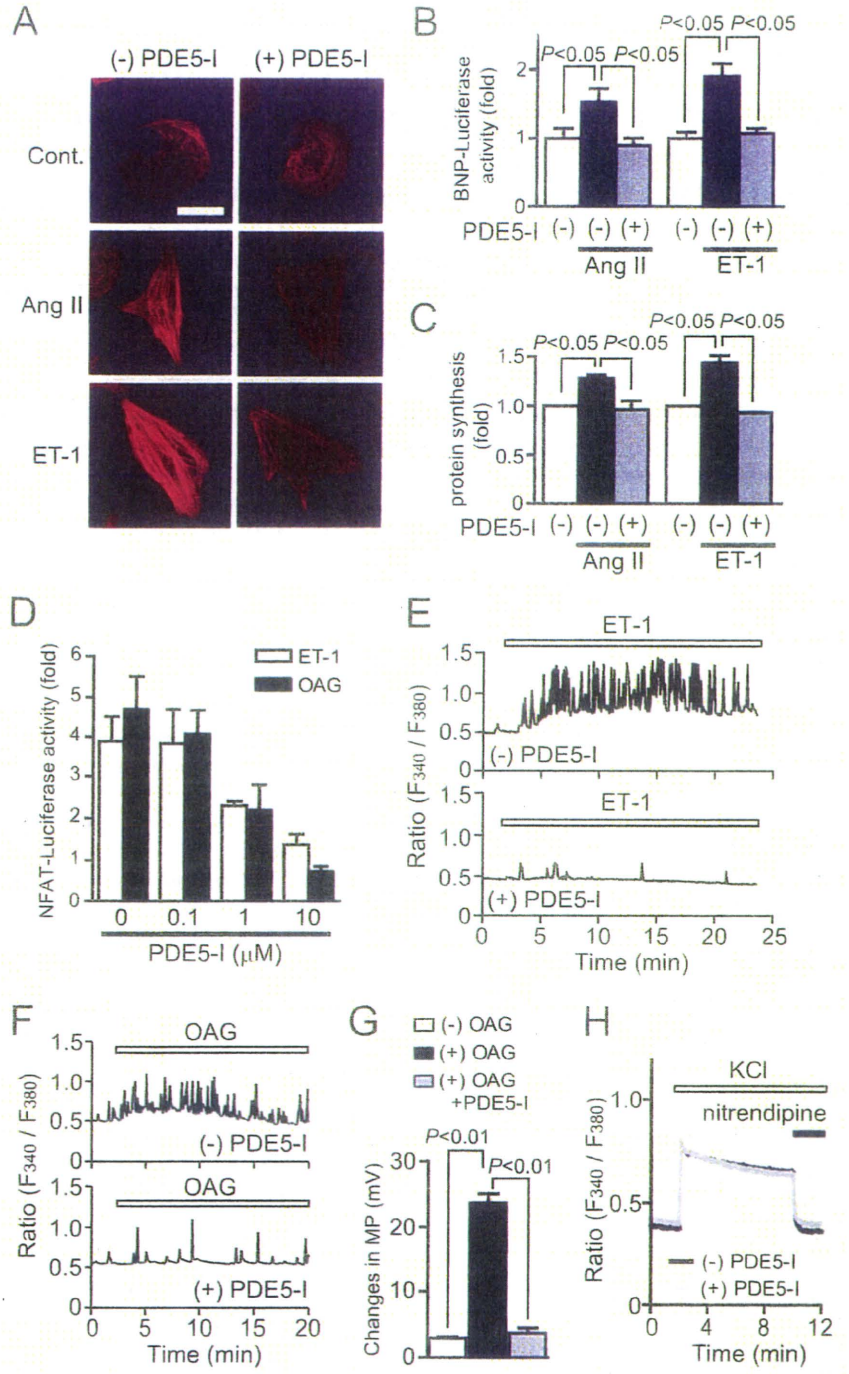

FIGURE 1. **Inhibition of PDE5 suppresses agonist-induced cardiomyocyte hypertrophic responses through inhibition of DAG-mediated Ca^{2+} signaling.** *A–C*, effects of PDE5-I on agonist-induced hypertrophic responses (actin reorganization (*A*), BNP expression (*B*), and protein synthesis (*C*)). Cardiomyocytes were treated with PDE5-I (10 μM) for 20 min before the addition of Ang II (1 μM) or ET-1 (100 nM). *Scale bar*, 50 μm. *D*, effects of PDE5-I on NFAT activation induced by ET-1 and OAG (30 μM). *E–H*, average time courses of Ca^{2+} responses induced by ET-1 (*E*), OAG (*F*), and KCl (*H*) in the absence or presence of PDE5-I. *G*, effects of PDE5-I on OAG-induced increase in membrane potential (*MP*). Cardiomyocytes were treated with OAG for 20 min, and maximal increase in MP was calculated from peak changes in $DiBAC_4(3)$ fluorescence intensity (21). *H*, voltage-dependent Ca^{2+} influx was evoked by KCl (8 mM) for 8 min, and nitrendipine (10 μM) was added to inhibit the activities of voltage-dependent Ca^{2+} channels.

only as a Ca^{2+}-permeable channel-forming subunit but also as an accessory protein to form the Ca^{2+} signaling complex (18). Endogenous TRPC1 and TRPC3 proteins are associated with each other to form native store-operated channels in HEK293 cells (19). In addition, diacylglycerol (DAG)-sensitive TRPC3, TRPC6, and TRPC7 proteins assemble to homotetramers or heterotetramers that function as DAG-activated cation channels (20). We have previously reported that TRPC3 and TRPC6 mediate Ang II-induced membrane depolarization, followed by Ca^{2+} influx through voltage-dependent Ca^{2+} channels in rat neonatal cardiomyocytes (21). Either knockdown of TRPC3 or TRPC6 channels completely suppressed Ang II-induced hypertrophy. Thus, TRPC1, TRPC3, and TRPC6 may form multimers in cardiomyocytes, which function as DAG-activated cation channels. Furthermore, we have recently demonstrated that treatment with a TRPC3 channel-selective blocker suppresses mechanical stretch-induced NFAT activation and pressure overload-induced cardiac hypertrophy in mice (22). Thus, inhibition of TRPC3-containing multimeric channels may represent a novel therapeutic strategy for preventing cardiac hypertrophy.

Phosphorylation of TRPC channels has been reported to modulate channel activity (23–25). For example, Fyn, an Src family Tyr kinase, physically interacts with the N-terminal region of TRPC6 proteins, and Tyr phosphorylation of TRPC6 enhances its channel activity (23). It has also been demonstrated that Src-dependent Tyr phosphorylation of TRPC3 is essential for DAG-activated cation influx (24). In contrast, Ser/Thr phosphorylation of TRPC3 channel attenuates its channel activity (25). Activation of PKG is known to regulate $[Ca^{2+}]_i$ at multiple levels (26). PKG activation by a NO donor or cGMP analog has been reported to inhibit voltage-dependent L-type Ca^{2+} channels by α_1-adrenergic receptor stimulation in cardiomyocytes (27). Several reports have shown that TRPC3 and TRPC6 channel activities are greatly attenuated by PKG-catalyzed phosphorylation of TRPC6 at threonine 69 (Thr^{69}) and TRPC3 at Thr^{11} and Ser^{263} (25, 28). The physiological importance of negative regulation of TRPC6 channels by the NO-

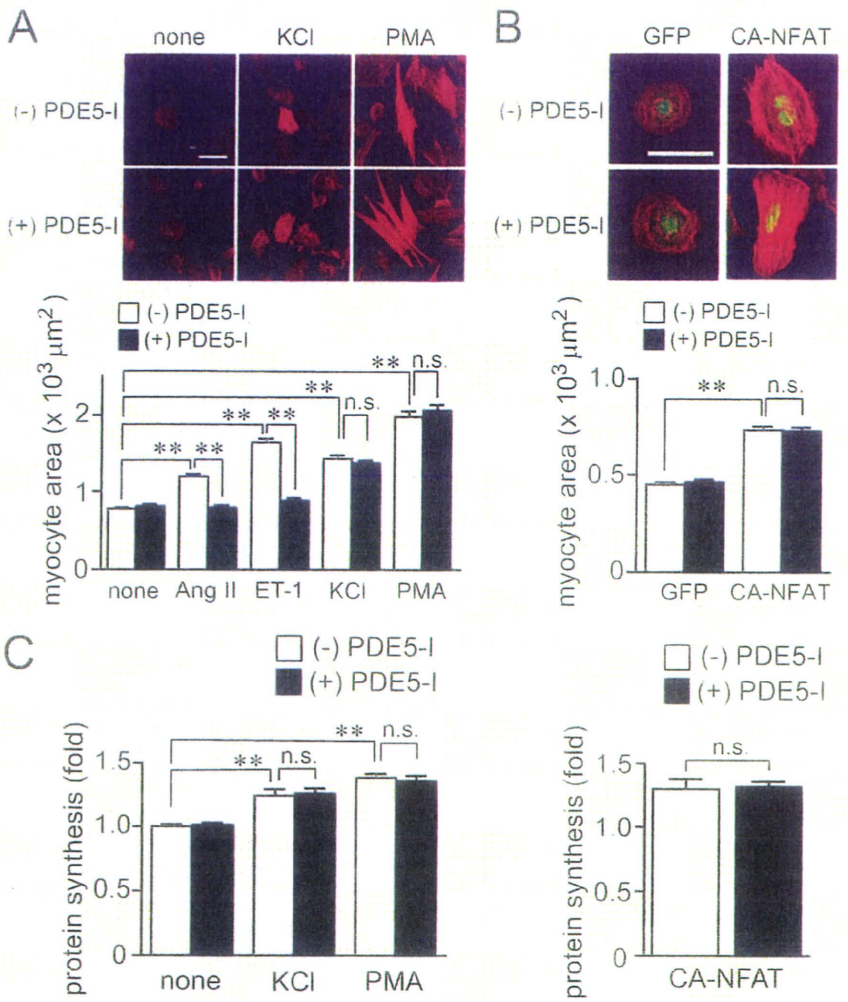

FIGURE 2. **Inhibition of PDE5 does not suppress the agonist-independent cardiomyocyte hypertrophic responses.** *A* and *C*, effects of PDE5-I on hypertrophic responses (actin reorganization, protein synthesis, and increases in area of cardiomyocytes) induced by KCl and phorbol 12-myristrate 13-acetate (*PMA*). Cardiomyocytes were stimulated with Ang II (1 μM), ET-1 (100 nM), KCl (5 mM), or phorbol 12-myristrate 13-acetate (1 μM) for 48 h. *B* and *C*, effects of PDE5-I on hypertrophic growth (*B*) and protein synthesis (*C*) in green fluorescent protein- and CA-NFAT-expressing cardiomyocytes. *Scale bar*, 50 μm. **, $p < 0.01$; *n.s.*, no significance.

cGMP-protein kinase G (PKG) signaling pathway has been reported in vascular smooth muscle cells (28). However, the role of PKG-dependent negative regulation of TRPC6 channels in the heart is still unknown.

Inhibition of cGMP-dependent phosphodiesterase 5 (PDE5) enhances basal PKG activity through an increase in intracellular cGMP concentration. In fact, chronic treatment with sildenafil, a PDE5 inhibitor, exhibits the anti-hypertrophic effects in mice (29, 30) and in patients with systolic heart failure (31). It has been reported that RGS2 mediates cardiac compensation to pressure overload and anti-hypertrophic effects of PDE5 inhibition in mice (32). Because PKG-dependent phosphorylation of RGS2 enhances GTPase activity of the α-subunit of G_q protein ($G\alpha_q$), this may explain the cGMP-dependent disruption of intracellular Ca^{2+} signaling induced by G_q-coupled receptor stimulation. However, we here found that inhibition of PDE5 also suppresses Ca^{2+} responses induced by the DAG analog and mechanical stretch (which may not require the activation of $G\alpha_q$ signaling) in rat neonatal cardiomyocytes. We also demonstrate that inhibition of PDE5 actually induces phosphorylation of TRPC6 proteins at Thr^{69}, leading to inhibition of TRPC6-mediated Ca^{2+} signaling. These results suggest that PKG-dependent inhibition of TRPC6 channel activity is required for the anti-hypertrophic effects of PDE5 inhibition.

EXPERIMENTAL PROCEDURES

Materials and Cell Cultures—A PDE5-selective inhibitor (PDE5-I; 4-{[3′,4′-(methylenedioxy)benzyl]amino}-6-methoxyquinazoline), 4-methyl-4′-[3,5-bis(trifluoromethyl)-1H-pyrazol-1-yl]-1,2,3-thiadiazole-5-carboxanilide (BTP2), and KT5823 were purchased from Calbiochem. 8-Bromo-cGMP (8-Br-cGMP), phorbol 12-myristrate 13-acetate, *S*-nitroso-*N*-acetyl-DL-penicillamine, 1-oleoyl-2-acetyl-*sn*-glycerol (OAG), and ET-1 were from Sigma. Ang II was from Peptide Lab. Fura2/AM was from Dojindo. Bis(1,3-dibutylbarbituric acid)trimethine oxonol ($DiBAC_4(3)$) was from Molecular Probes. Collagenase and Fugene 6 were from Roche Applied Science. Stealth small interfering RNA (siRNA) oligonucleotides, Alexa Fluor 568 phalloidin, and Lipofectamine 2000 were purchased from Invitrogen. Revatio (sildenafil citrate) was from Pfizer. The cDNAs coding a dominant negative mutant of TRPC6 (DN-TRPC6) and the TRPC6 (T69A) mutant were constructed as described (21, 28). Anti-TRPC6 was from Alomone. Phospho-Thr^{69} TRPC6 antiserum was generated against phospho-TRPC6 peptide (CHRRQ(P)TILREK). The phospho-TRPC6 antibody was purified by an antigen column. Isolation of rat neonatal cardiomyocytes and adenoviral infection of LacZ, green fluorescent protein, wild type (WT) TRPC6, or DN-TRPC6 were described (33). For knockdown of rat RGS proteins, cells were transfected with siRNAs (100 nM each) for RGS2 (AGAAAUAGCUCAAACGGGUCUUCCA) and RGS4 (UUUGAAAGCUGCCAGUCCACAUUCA) or control scrambled siRNAs for RGS2 (UUCACGGAACCGACCUUAAAUA) and RGS4 (AAAUAGCGUCUGACCACCCUUAGGU), using Lipofectamine 2000 for 72 h.

Reporter Activity—Measurement of NFAT-dependent luciferase activity and brain natriuretic peptide (BNP) promoter activity was performed as described previously (21). Briefly, cardiomyocytes (5×10^5 cells) plated on 24-well

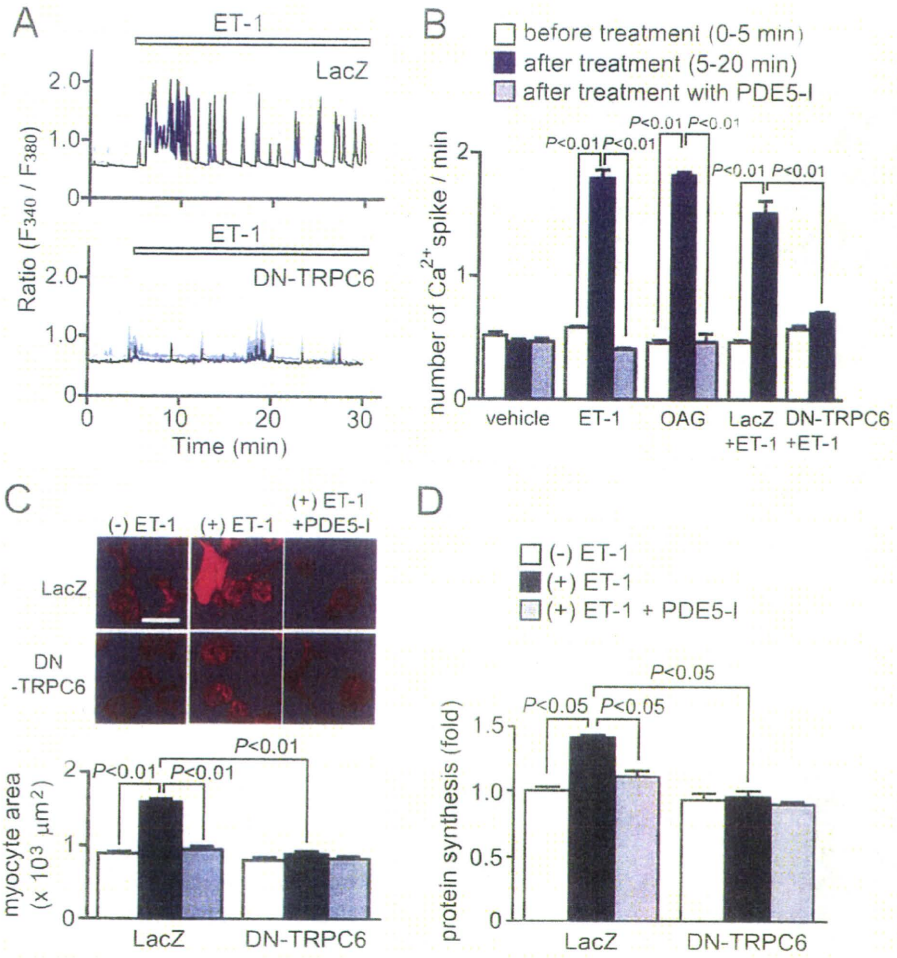

FIGURE 3. **TRPC6 mediates ET-1-induced cardiomyocyte hypertrophic responses.** *A*, Ca^{2+} responses induced by ET-1 (100 nM) in LacZ- and DN-TRPC6-overexpressing cardiomyocytes. *B*, results of the frequency of Ca^{2+} oscillations induced by ET-1 or OAG (30 μM). Cardiomyocytes were pretreated with PDE5-I (10 μM) 35 min before agonist stimulation. *C* and *D*, effects of DN-TRPC6 on ET-1-induced actin reorganization and increase in cell size (*C*) and protein synthesis (*D*). *Scale bar*, 50 μm.

dishes were transiently co-transfected with 0.45 μg of pNFAT-Luc and 0.05 μg of pRL-SV40 control plasmid or with 0.3 μg of pBNP-Luc and 0.2 μg of pRL-SV40 using Fugene 6. Expression of the constitutively active mutant of green fluorescent protein-fused NFAT proteins (CA-NFAT) was performed as described (34). Forty-eight h after transfection, cells were stimulated with Ang II (1 μM), ET-1 (100 nM), or mechanical stretch (21) for 6 h (for NFAT) or 24 h (for BNP).

Measurement of $[Ca^{2+}]_i$ and Membrane Potential—The intracellular Ca^{2+} concentration ($[Ca^{2+}]_i$) of cardiomyocytes or HEK293 cells was determined as described (35, 36). Briefly, HEK293 cells were transfected for 48 h with vector (pCI-neo), WT TRPC6, or TRPC6 (T69A) mutant using Fugene 6. Cardiomyocytes (1×10^6 cells) were plated on gelatin-coated glass bottom 35-mm dishes or on laminin-coated silicone rubber culture dishes (4 cm^2; STREX) and were loaded with 1 μM fura-2/AM at 37 °C for 30 min (37). As we measured the changes in $[Ca^{2+}]_i$ of the same cells before and after mechanical stretch, we treated cells with 20% of transient stretch for 3 s using automatic stretch systems (STB-150; STREX). Measurement and analysis of membrane potential were performed using $DiBAC_4(3)$ as described (21). The fluorescence intensity was measured with a video image analysis system (Aquacosmos, Hamamatsu Photonics).

Animal Models and Drug Treatment—All experiments on male C57BL6/J mice (C57BL6/J) were performed in accordance with the Guide for the Care and Use of Laboratory Animals prepared by Kyushu University. Sildenafil (100 mg/kg/day) was orally administered once a day for 1 week, and then hearts were removed and homogenized with radioimmune precipitation buffer.

Western Blot Analysis—TRPC6-expressing HEK293 cells (3×10^5 cells) or cardiomyocytes (1×10^6 cells) plated on 6-well dishes were directly harvested with 2× SDS sample buffer (200 μl). After centrifugation, supernatants (20–40 μl) were fractionated by 8% SDS-polyacrylamide gel and then transferred onto polyvinylidene difluoride membrane. For measurement of TRPC6 phosphorylation in mouse hearts, supernatants (100 μg of proteins) without boiling treatment were applied onto SDS-polyacrylamide gel. The expression and phosphorylation of endogenous TRPC6 proteins were detected by anti-TRPC6 (dilution rate, 1:1000) and anti-phospho-TRPC6 (1:1000) antibodies. We visualized the reactive bands using Supersignal® West Pico Luminol/Enhancer solution (Pierce). The optical density of the film was scanned and measured with Scion Image software.

Measurement of Hypertrophic Responses of Cardiomyocytes—Measurement of cardiomyocyte hypertrophy was performed as described (21, 34). Cardiomyocytes were fixed by paraformaldehyde and then stained with Alexa Fluor 548 phalloidin to visualize actin filaments. Digital photographs were taken at ×600 magnification with confocal microscopy (FV-10i, Olympus) or a Biozero microscope (BZ-8000, Keyence), and the average values of the cardiomyocyte area ($n > 100$ cells) were calculated using a BZ-II analyzer (Keyence). Protein synthesis was measured by [^{3}H]leucine incorporation. After cells were stimulated with Ang II or ET-1 for 2 h, [^{3}H]leucine (1 μCi/ml) was added to the culture medium and further incubated for 6 h. The incorporated [^{3}H]leucine was measured using a liquid scintillation counter.

Statistical Analysis—The results are shown as means ± S.E. All experiments were repeated at least three times. Statisti-

cal comparisons were made with a two-tailed Student's *t* test or analysis of variance followed by the Student-Newman-Keuls procedure with significance imparted at p values of <0.05.

RESULTS

Suppression of Diacylglycerol-mediated Ca^{2+} Responses by Inhibition of PDE5—We first investigated whether inhibition of PDE5 suppresses agonist-induced Ca^{2+} responses and hypertrophic responses in rat cardiomyocytes. Treatment with PDE5-I completely suppressed Ang II- or ET-1-induced hypertrophic responses, such as an increase in cell size, actin reorganization, hypertrophic gene (BNP) expression, and protein synthesis (Fig. 1, *A–C*). Stimulation of cardiomyocytes with ET-1 increases the frequency of Ca^{2+} oscillations through voltage-dependent Ca^{2+} channels (38). PDE5-I also suppressed ET-1-induced NFAT activation and oscillatory and sustained increase in $[Ca^{2+}]_i$ (Fig. 1, *D* and *E*). Although expression of CA-NFAT increased NFAT activity about 2.5-fold, this NFAT activation was not suppressed by PDE5-I (data not shown). These results suggest that PDE5-I inhibits NFAT activity through inhibition of Ca^{2+} responses. We have previously shown that DAG-sensitive TRPC channels (TRPC3 and TRPC6) mediate Ang II-induced activation of voltage-dependent Ca^{2+} influx through membrane depolarization (21). Treatment with OAG increased NFAT activity and the frequency of Ca^{2+} spikes, which were suppressed by PDE5-I (Fig. 1, *D* and *F*). In addition, the OAG-induced membrane depolarization, as determined by $DiBAC_4(3)$ imaging, was completely suppressed by PDE5-I pretreatment (Fig. 1*G*). Furthermore, nitrendipine-sensitive voltage-dependent Ca^{2+} influx-mediated increase in $[Ca^{2+}]_i$ induced by high KCl was not affected by PDE5-I pretreatment (Fig. 1*H*). In addition, the hypertrophic responses induced by high KCl (Fig. 2, *A* and *C*) or the expression of CA-NFAT (Fig. 2*B*) were not suppressed by PDE5 inhibition. Although DAG also activates protein kinase C-dependent hypertrophic signaling pathway (3), PDE5-I did not suppress the phorbol 12-myristrate 13-acetate-induced hypertrophic responses (Fig. 2, *A* and *C*). These results suggest that PDE5-I suppresses agonist-induced Ca^{2+} responses and cardiomyocyte hypertrophy through inhibition of DAG-mediated membrane depolarization.

Inhibition of TRPC6 Channel Activity by PDE5 Inhibition—To investigate the involvement of TRPC6 in agonist-induced cardiomyocyte hypertrophy, we used DN-TRPC6 (21). As shown in Fig. 3*A*, treatment of cardiomyocytes with ET-1 or OAG significantly increased the frequency of Ca^{2+} spikes, which were completely suppressed by PDE5 inhibition (Fig. 3, *A* and *B*). Expression of DN-TRPC6 also completely suppressed ET-1-induced increases in the frequency of Ca^{2+} spikes (Fig. 3, *A* and *B*) and hypertrophic responses (Fig. 3, *C* and *D*). The anti-hypertrophic effect of PDE5-I was completely abolished in DN-TRPC6-expressing myocytes, suggesting that PDE5-I suppresses the TRPC6-mediated hypertrophic signaling pathway.

Takahashi *et al.* (28) have recently reported that activation of the NO-cGMP-PKG pathway by extracellular treatment with a NO donor or cGMP analog inhibits TRPC6 channel activity through phosphorylation of TRPC6 at Thr^{69}. Thus, we next examined whether PDE5 inhibition attenuates TRPC6 channel activity. Compared with vector-expressing HEK293 cells, treatment with OAG induced a marked increase in $[Ca^{2+}]_i$ of TRPC6-expressing cells (Fig. 4*A*). The TRPC6-mediated increase in $[Ca^{2+}]_i$ was significantly suppressed by pretreatment with PDE5-I as well as *S*-nitroso-*N*-acetyl-DL-penicillamine and 8-Br-cGMP (Fig. 4*B*). The IC_{50} value of inhibition of the TRPC6-mediated increase in $[Ca^{2+}]_i$ by PDE5-I was 0.41 ± 0.08 μM (Fig. 4*C*). More than 15 min of pretreatment with PDE5-I was required for the suppression of the TRPC6-mediated increase in $[Ca^{2+}]_i$ induced by OAG (Fig. 4*D*). PDE5-I suppressed the Ca^{2+} influx-mediated increase in $[Ca^{2+}]_i$ induced by OAG in TRPC6 (WT)-expressing cells, which was completely abolished by co-treatment with a PKG-selective inhibitor, KT5823 (Fig. 4, *E* and *F*). These results suggest that activation of PKG is required for the inhibition of TRPC6 channel activity. In fact, the suppression of OAG-induced Ca^{2+} influx by PDE5-I treatment was abolished in TRPC6 (T69A)-expressing cells. Thus, PKG-dependent phosphorylation of TRPC6 at Thr^{69} may be essential for inhibition of TRPC6 channel activity by PDE5 inhibition.

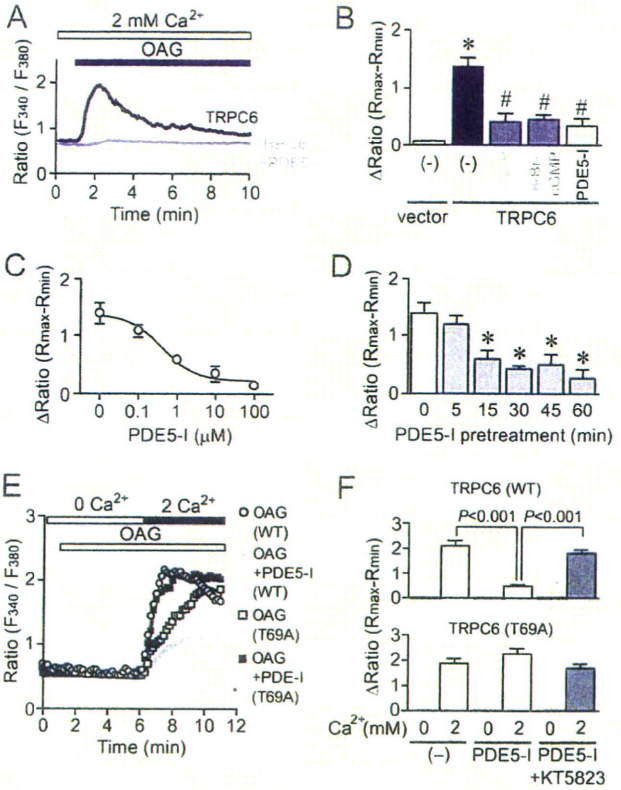

FIGURE 4. **PKG-dependent suppression of TRPC6-mediated Ca^{2+} influx by PDE5 inhibition.** *A*, average time courses of Ca^{2+} responses induced by OAG (30 μM) in vector and TRPC6-expressing HEK293 cells with or without PDE5-I. *B*, peak increases in $[Ca^{2+}]_i$ induced by OAG in vector- and TRPC6-expressing cells. HEK293 cells were treated with *S*-nitroso-*N*-acetyl-DL-penicillamine (*SNAP*) (100 μM), 8-Br-cGMP (100 μM), or PDE5-I (10 μM) for 30 min before the addition of OAG (30 μM). *C* and *D*, concentration-dependent (*C*) and time-dependent (*D*) suppression of OAG-induced $[Ca^{2+}]_i$ increases by PDE5-I. *E* and *F*, effects of PDE5-I on OAG-induced Ca^{2+} influx-mediated $[Ca^{2+}]_i$ increases in TRPC6 (WT)- and TRPC6 (T69A)-expressing cells. HEK293 cells were treated with KT5823 (1 μM) for 30 min before the addition of OAG. *, $p < 0.05$ *versus* vector (*white bar*); #, $p < 0.05$ *versus* TRPC6 (−) control (*black bar*).

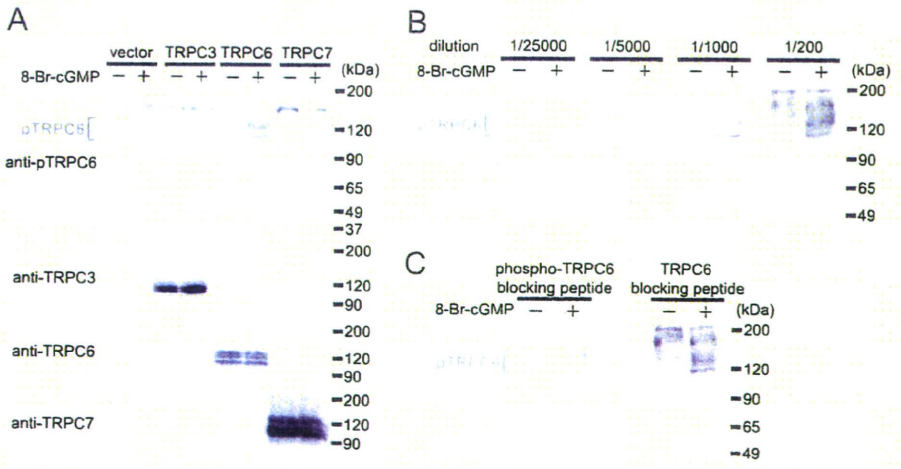

FIGURE 5. **Specific recognition of TRPC6 phosphorylation at Thr^{69} by a phospho-specific antibody.** *A*, phosphorylation of TRPC6 at Thr^{69} induced by PKG activation in vector-, TRPC3-, TRPC6-, and TRPC7-expressing HEK293 cells. HEK293 cells were treated with 8-Br-cGMP (100 μM) for 2 h. *B*, optimization of dilution of anti-phospho-TRPC6 antibody. Antibody (0.56 mg/ml) was diluted with Tris-buffered saline plus 0.1% Tween 20 (TBS-T) and incubated with blots for 1 h at room temperature. *C*, effect of treatment with a TRPC6-blocking peptide on the recognition of TRPC6 phosphorylation by this antibody. Blots were incubated with phospho-TRPC6 antibody diluted 1:1000 in TBS-T with phospho-TRPC6-blocking peptide or non-phosphorylated TRPC6-blocking peptide (10 μg/ml) for 1 h at room temperature.

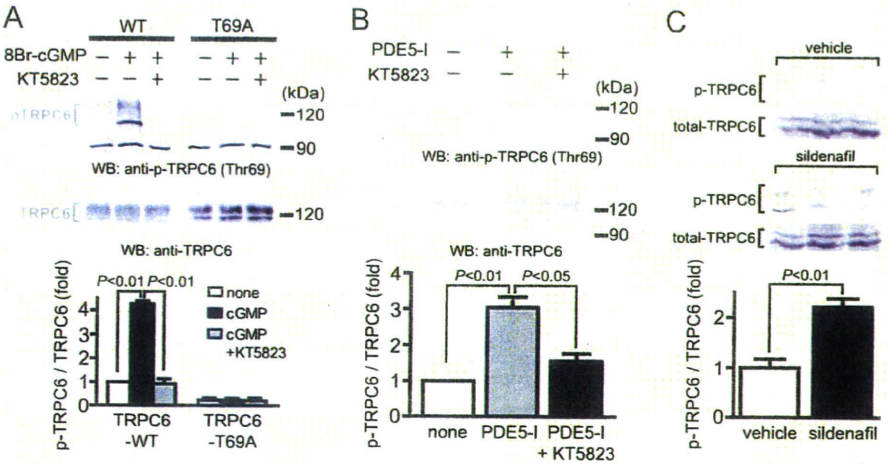

FIGURE 6. **PKG-dependent phosphorylation of Thr^{69} in TRPC6 by PDE5 inhibition.** *A*, PKG-dependent phosphorylation of TRPC6 proteins at Thr^{69} in TRPC6 (WT)- and TRPC6 (T69A)-expressing HEK293 cells. HEK293 cells were treated with KT5823 (1 μM) for 20 min before the addition of 8-Br-cGMP (100 μM) and PDE5-I (10 μM) for 30 min. *B*, PKG-dependent TRPC6 phosphorylation by PDE5-I. Cardiomyocytes were treated with KT5823 for 20 min before the addition of PDE5-I (10 μM) for 1 h. *C*, effects of sildenafil on the phosphorylation of TRPC6 in mice. One week after oral administration with sildenafil (100 mg/kg/day), hearts were lysed with radioimmune precipitation buffer, and 100 μg of proteins were applied to SDS-PAGE.

Phosphorylation of TRPC6 Proteins at Thr^{69} by PDE5 Inhibition—In order to examine whether inhibition of PDE5 actually induces phosphorylation of TRPC6 proteins in cardiomyocytes, we generated a phospho-specific TRPC6 (Thr^{69}) antibody. Because TRPC6 proteins have two glycosylation sites (39), a single 100 kDa band and smear 110–120 kDa bands due to several patterns of glycosylation were observed in TRPC6 wild type (WT)-overexpressing HEK293 cells (Fig. 5*A*). Phosphorylation of TRPC6 proteins was observed only when HEK293 cells were stimulated with 8-Br-cGMP. In contrast, this phosphorylation was not observed in vector-, TRPC3-, or TRPC7-expressing HEK293 cells, even when cells were stimulated with 8-Br-cGMP. The TRPC6 phosphorylation could be detectable when the antibody was diluted from 1,000- to 5,000-fold (Fig. 5*B*). Furthermore, the TRPC6 phosphorylation bands were completely abolished by the treatment with phospho-TRPC6-blocking peptide but not by control blocking peptide (Fig. 5*C*). These results clearly suggest that our phospho-specific TRPC6 antibody specifically recognized the phosphorylation of rodent TRPC6 at Thr^{69}.

Activation of PKG by 8-Br-cGMP and PDE5-I stimulated the phosphorylation of TRPC6 proteins, which was completely suppressed by the treatment with KT5823 in TRPC6-WT-expressing HEK293 cells (Fig. 6, *A* and *B*). The PKG-mediated TRPC6 phosphorylation was not observed in TRPC6 (T69A)-expressing cells, indicating the specificity of this antibody. Treatment with PDE5-I significantly increased the phosphorylation of native TRPC6 proteins in rat cardiomyocytes, which was completely suppressed by KT5823 (Fig. 6*B*). We further examined whether inhibition of PDE5 actually phosphorylates TRPC6 proteins *in vivo*. Takimoto *et al.* (29) have previously reported that chronic treatment with sildenafil (100 mg/kg/day) prevents and reverses cardiac hypertrophy induced by pressure overload in mice. We found that oral treatment with sildenafil (100 mg/kg/day) for 1 week, under the same conditions as in their report, actually increases TRPC6 phosphorylation levels in mouse hearts (Fig. 6*C*).

Inhibition of TRPC6 Phosphorylation at Thr^{69} Diminishes the Anti-hypertrophic Effects of PDE5 Inhibition—Overexpression of TRPC6 (T69A) enhanced the increase in NFAT activity and BNP expression induced by ET-1, which was not suppressed by PDE5-I (Fig. 7, *A* and *B*). In addition, expression of TRPC6 (WT) or TRPC6 (T69A) enhanced the ET-1-induced hypertrophic responses of cardiomyocytes (Fig. 7, *C* and *D*). Although PDE5-I completely suppressed the ET-1-induced hypertrophic responses in control (vector)- or TRPC6 (WT)-expressing cardiomyocytes, PDE5-I did not suppress hypertrophic responses in TRPC6 (T69A)-expressing cardiomyocytes. These results suggest that inhibition of TRPC6 channel activity via its PKG-dependent phosphorylation at Thr^{69} participates in anti-cardiomyocyte hypertrophic effects of PDE5 inhibition.

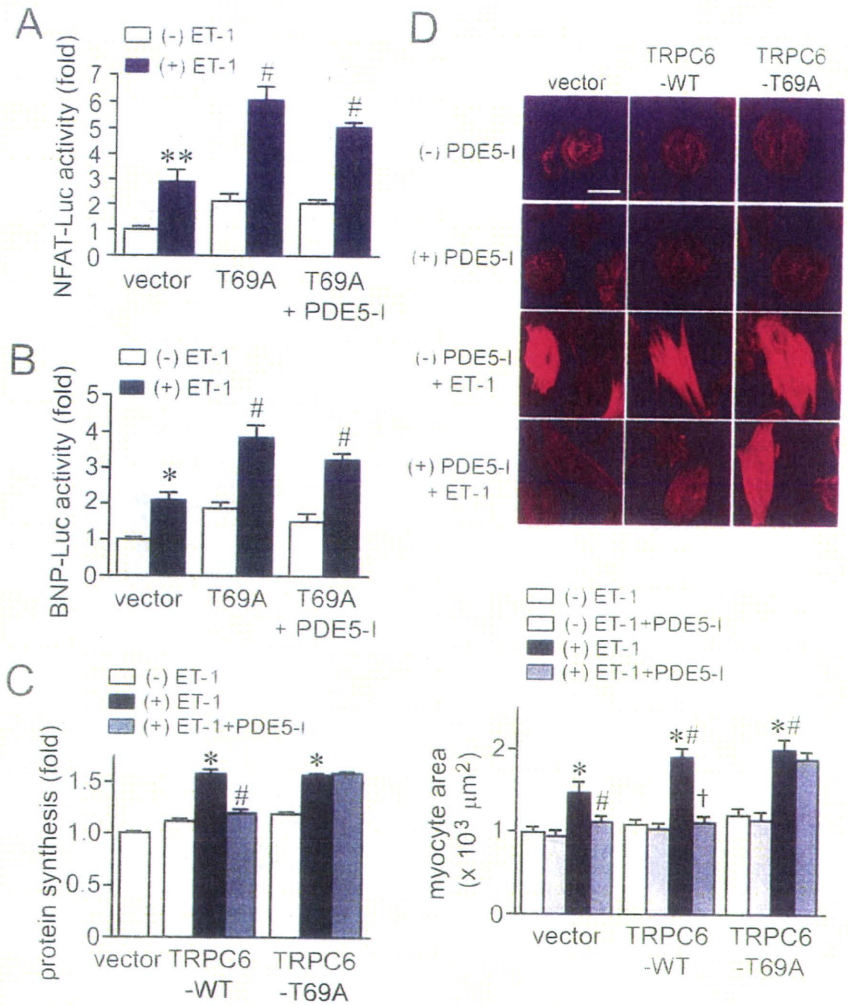

FIGURE 7. **Phosphorylation of Thr^{69} is essential for the anti-hypertrophic effects of PDE5 inhibition.** *A* and *B*, effects of PDE5-I on ET-1-induced NFAT activation (*A*) and BNP gene expression (*B*) in TRPC6 (T69A)-expressing cardiomyocytes. *C* and *D*, effects of PDE5-I on the ET-1-induced protein synthesis (*C*) and increase in the size of TRPC6 (T69A)-overexpressing cardiomyocytes (*D*). Cardiomyocytes were treated with PDE5-I (10 μM) for 20 min before the addition of ET-1 (100 nM). *Scale bar*, 50 μm. *, $p < 0.05$; **, $p < 0.01$ *versus* without (−) ET-1 within vector. #, $p < 0.05$ *versus* vector with (+) ET-1. †, $p < 0.01$ *versus* TRPC6-WT with ET-1.

Suppression of Mechanical Stretch-induced Ca^{2+} Responses by PDE5 Inhibition—Because mechanical stress is also involved in the development of cardiac hypertrophy, we next examined whether PDE5-I inhibits Ca^{2+} responses induced by mechanical stretch. In control cardiomyocytes, a periodic increase in $[Ca^{2+}]_i$ was observed after cells were stretched by 20% for 3 s with a speed of 20 mm/s (Fig. 8*A*). A bis(trifluoromethyl)pyrazole derivative, BTP2, is recently used as a selective inhibitor of the TRPC1 to -7 channels. We previously reported that BTP2 at 3 μM suppresses TRPC6-mediated Ca^{2+} influx by 80% in HEK293 cells (22). Treatment with PDE5-I or BTP2 abolished mechanical stretch-induced increase in $[Ca^{2+}]_i$ (Fig. 8*A*). Mechanical stretch-induced increases in NFAT-dependent luciferase activity, BNP-luciferase activity, and protein synthesis were suppressed by PDE5-I, which was canceled by co-treatment with KT5823 (Fig. 8, *B–D*). We also found that mechanical stretch-induced increases in $[Ca^{2+}]_i$, NFAT activation, and hypertrophic responses were completely suppressed by the expression of DN-TRPC6 (Fig. 8, *B–D*). These results suggest that PDE5-I suppresses mechanical stretch-induced Ca^{2+} responses linked to cardiomyocyte hypertrophic responses through inhibition of TRPC6 channels.

Knockdown of RGS2 and RGS4 Does Not Affect the Effect of PDE5-I—It has been recently reported that PKG-dependent phosphorylation of RGS2 and RGS4 mediates the anti-hypertrophic effects in mouse hearts (32, 40, 41). Thus, we next examined the involvement of RGS proteins in the inhibition of agonist-induced Ca^{2+} responses by PDE5 inhibition, using siRNAs for RGS2 and RGS4. We confirmed that the treatment of cardiomyocytes with siRNAs for RGS2/4 reduced the expression levels of RGS2 and RGS4 mRNAs to 18.5 ± 5.2 and 26.7 ± 7.8%, respectively. Knockdown of RGS2/4 proteins did not affect Ca^{2+} responses and NFAT activation induced by ET-1 (Fig. 9). The addition of extracellular Ca^{2+} induced a Ca^{2+} influx-mediated increase in $[Ca^{2+}]_i$ by ET-1 stimulation, which was significantly suppressed by PDE5-I treatment in control myocytes (Fig. 9, *A–C*). The Ca^{2+} influx-mediated $[Ca^{2+}]_i$ increases and increase in NFAT activity by agonist stimulation were slightly enhanced in RGS2/4-deficient myocytes and were also significantly suppressed by PDE5-I treatment (Fig. 9, *B–D*). These results suggest that RGS2 and RGS4 proteins are not mainly involved in the inhibition of agonist-induced Ca^{2+} responses by PDE5 inhibition in cardiomyocytes.

DISCUSSION

In this study, we have demonstrated that inhibition of PDE5 suppresses agonist-induced and mechanical stretch-induced hypertrophic responses in rat cardiomyocytes. The increases in the frequency of Ca^{2+} oscillations induced by OAG or mechanical stretch are greatly attenuated by PDE5 inhibition. PDE5-I suppresses OAG-induced membrane depolarization, suggesting the inhibition of DAG-sensitive TRPC channels by PDE5 inhibitor. Treatment with PDE5-I actually induces PKG-dependent phosphorylation of TRPC6 proteins at Thr^{69} and inhibits TRPC6-mediated Ca^{2+} responses. Because the inhibition of ET-1-induced hypertrophic responses by PDE5-I was abolished in TRPC6 (T69A)-expressing cardiomyocytes, we suggest that phosphorylation of TRPC6 is required for

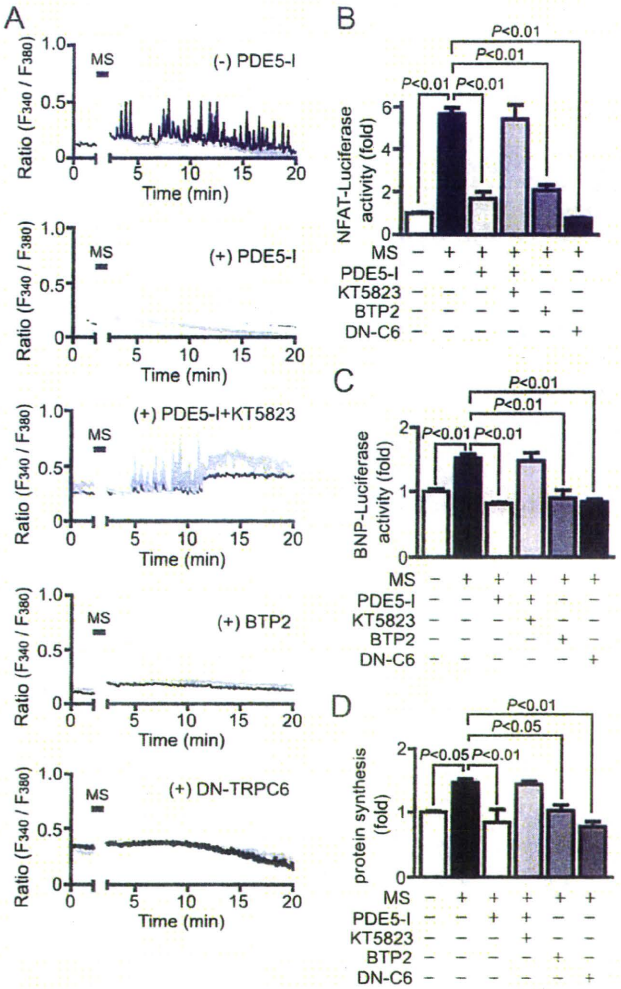

FIGURE 8. **Inhibition of PDE5 suppresses Ca^{2+} responses and cardiomyocyte hypertrophic responses induced by mechanical stretch.** *A*, typical traces of Ca^{2+} responses induced by mechanical stretch (*MS*) in the absence or presence of PDE5-I, KT5823, or BTP2. Cardiomyocytes were treated with PDE5-I (10 μM) or BTP2 (5 μM) for 35 min before MS. DN-TRPC6 proteins were expressed using adenoviral infection. *B–D*, effects of PDE5-I, BTP2, and DN-TRPC6 on the MS-induced NFAT activation (*B*) and hypertrophic responses (BNP gene expression (*C*) and protein synthesis (*D*)).

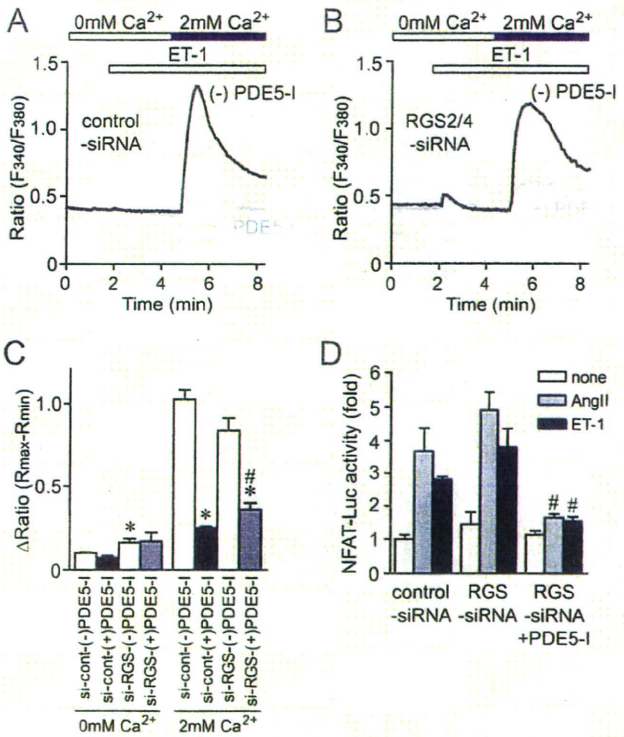

FIGURE 9. **PDE5-I suppresses ET-1-induced Ca^{2+} responses in RGS2/4-down-regulated cardiomyocytes.** *A* and *B*, average time courses of Ca^{2+} responses induced by ET-1 in the absence or presence of PDE5-I in control siRNA-treated cardiomyocytes (*A*) and RGS2/4 siRNAs-treated cardiomyocytes (*B*). *C*, peak Ca^{2+} releases (0 mM Ca^{2+}) and Ca^{2+} influx-mediated increases in $[Ca^{2+}]_i$ (2 mM Ca^{2+}) induced by ET-1 (100 nM). *D*, effects of knockdown of RGS2/4 proteins on PKG-dependent inhibition of ET-1-induced NFAT activation by PDE5-I. *, $p < 0.05$ *versus* control siRNA-treated cardiomyocytes without PDE5-I; #, $p < 0.05$ *versus* RGS2/4 siRNA-treated cardiomyocytes without PDE5-I.

the anti-hypertrophic effects of PDE5 inhibition. In addition, PDE5-I-induced suppression of Ca^{2+} influx induced by ET-1 was not abolished by the knockdown of RGS2 and RGS4, both of which are reported to be activated by PKG. This result emphasizes the physiological importance of TRPC6 phosphorylation by PDE5-I in suppressing Ca^{2+} influx induced by agonist stimulation and mechanical stretch.

Higazi *et al.* (38) has recently reported that inositol-1,4,5-trisphosphate-induced Ca^{2+} release from perinuclear inositol-1,4,5-trisphosphate receptors by ET-1 stimulation or membrane depolarization preferentially couples to the calcineurin/NFAT pathway to induce hypertrophy. They have also demonstrated that the potentiation of Ca^{2+} influx activity induced by isoproterenol or BayK8644 induces activation of calcineurin/NFAT signaling pathway via Ca^{2+} release from perinuclear inositol-1,4,5-trisphosphate receptors. This mechanism may be involved in the process of voltage-dependent Ca^{2+} influx-mediated NFAT activation evoked by TRPC6 activation. Although we did not measure nuclear Ca^{2+} concentrations, PDE5-I may inhibit the increase in nuclear Ca^{2+} concentrations because PDE5-I suppresses NFAT activation induced by ET-1.

Because PDE5-I did not suppress the high KCl-induced increase in $[Ca^{2+}]_i$ (Fig. 1), we suggest that PKG activation by PDE5-I does not inhibit L-type Ca^{2+} channels. In contrast, Fiedler *et al.* (27) have reported that overexpression of PKG type I suppresses single L-type Ca^{2+} channel open probability and $[Ca^{2+}]_i$ transient amplitude. This discrepancy can be explained by the intensity of PKG activation. Although we show that PDE5-I increased the TRPC6 phosphorylation level about 3-fold, the treatment with 8-Br-cGMP induced a more than 5-fold increase in TRPC6 phosphorylation level (data not shown). This suggests that PDE5-I moderately activates PKG, and this activation is insufficient to inhibit L-type Ca^{2+} channel activity.

Inhibition of PDE5 suppresses mechanical stretch-induced Ca^{2+} responses in cardiomyocytes. Because the pattern of Ca^{2+} spikes is similar to those induced by ET-1 or OAG stimulation, membrane depolarization may be also involved in this mechanism. This idea is supported by the reports that DAG-sensitive TRPC channels work as stretch-

activated depolarizing channels in the vascular system (42–44). It has recently been reported that TRPC6 is activated by mechanical stretch through two pathways: G protein-mediated indirect activation and direct activation of TRPC6 (42). Furthermore, TRPC6 can be synergistically activated by mechanical force in the presence of G_q-coupled receptor stimulation (43). We have previously reported that mechanical stretch increases the concentration of extracellular nucleotides, which stimulate G_q protein-coupled P2Y receptors (37). Thus, extracellular nucleotides released by mechanical stretch and mechanical force may synergistically increase TRPC6 channel activity in rat neonatal cardiomyocytes.

Because Kwan *et al.* (25) reported that the activation of PKG by NO donor and 8-Br-cGMP increases phosphorylation at Thr^{11} and Ser^{263} of human TRPC3 proteins, it is possible that inhibition of PDE5 also results in phosphorylation of TRPC3 proteins and reduction of TRPC3 channel activity. Although Ser^{263} of human TRPC3 protein is conserved among humans, rats, and mice, Thr^{11} is not present in mouse and rat TRPC3 proteins. We have tried to generate an antibody to recognize the phosphorylated form of Ser^{263} in TRPC3 but failed to obtain the useful antibody. However, we confirmed that PDE5-I inhibits TRPC3-mediated Ca^{2+} influx induced by OAG in TRPC3-expressing HEK293 cells, which was abolished in TRPC3 (S325A)-expressing HEK293 cells (n = 2; data not shown). Because the Ser^{325} in mouse TRPC3 protein is identical to Ser^{263} in human TRPC3 protein, this result implies that the inhibition of TRPC3 channel activity by PDE-I may also be involved in the anti-hypertrophic effects of PDE5 inhibition.

We have not yet been able to identify the individual roles of TRPC6 and TRPC3 channels in cardiomyocytes. Despite their high degree of structural and functional similarity, TRPC3, TRPC6, and TRPC7 are substantially different in their basal channel activities (45). The basal channel activity of TRPC6 is tightly regulated (39). In contrast, TRPC3 and TRPC7 have considerable constitutive activity when expressed in various cell lines (46). Despite the low basal activity of TRPC6 channels, results from transgenic mice with cardiomyocyte-specific expression of TRPC3 or TRPC6 channels show that the up-regulation of TRPC6 channel proteins is essential for the development of cardiac hypertrophy (13, 14). In pathological conditions, hearts are exposed to mechanical stress and neurohumoral factors. Therefore, a characteristic of TRPC6 channels that is synergistically activated by mechanical stretch in the presence of a low concentration of agonist (43) may explain the mechanism of induction of pathological hypertrophy. Because TRPC3 has high constitutive activity among the DAG-activated TRPC3/6/7 family and is up-regulated in smooth muscle cells from TRPC6-deficient mice (45), the TRPC6-deficient mouse heart may cause excessive hypertrophy by pressure overload like a TRPC3-transgenic mouse heart (13). In addition, there is no pharmacological tool that selectively inhibits TRPC6 channel activity. Generation of transgenic mice with heart-specific expression of the dominant negative TRPC6 mutant, which moderately inhibits the function of TRPC6 channels without any compensation, will be necessary for understanding the pathophysiological role of TRPC6 in the heart.

In conclusion, we demonstrated that inhibition of DAG-sensitive TRPC channel activities through PKG-dependent phosphorylation is required for the anti-hypertrophic effects of PDE5 inhibition in rat cardiomyocytes. Our finding will provide a new insight for the creation of therapeutic strategies for heart failure.

Acknowledgments—We thank Marina Ariyoshi and Shinji Oda for measurement of Ca^{2+} imaging during the early stage of this study. We also thank Dr. Koichiro Kuwahara (Kyoto University) for helpful comments.

REFERENCES

1. Mann, D. L. (1999) *Circulation* **100,** 999–1008
2. Dorn, G. W., 2nd, and Force, T. (2005) *J. Clin. Invest.* **115,** 527–537
3. Heineke, J., and Molkentin, J. D. (2006) *Nat. Rev. Mol. Cell Biol.* **7,** 589–600
4. Liao, X. D., Tang, A. H., Chen, Q., Jin, H. J., Wu, C. H., Chen, L. Y., and Wang, S. Q. (2003) *Biochem. Biophys. Res. Commun.* **310,** 405–411
5. Molkentin, J. D., Lu, J. R., Antos, C. L., Markham, B., Richardson, J., Robbins, J., Grant, S. R., and Olson, E. N. (1998) *Cell* **93,** 215–228
6. Frey, N., McKinsey, T. A., and Olson, E. N. (2000) *Nat. Med.* **6,** 1221–1227
7. Ramirez, M. T., Zhao, X. L., Schulman, H., and Brown, J. H. (1997) *J. Biol. Chem.* **272,** 31203–31208
8. Song, K., Backs, J., McAnally, J., Qi, X., Gerard, R. D., Richardson, J. A., Hill, J. A., Bassel-Duby, R., and Olson, E. N. (2006) *Cell* **125,** 453–466
9. Berridge, M. J., Bootman, M. D., and Roderick, H. L. (2003) *Nat. Rev. Mol. Cell Biol.* **4,** 517–529
10. Colella, M., Grisan, F., Robert, V., Turner, J. D., Thomas, A. P., and Pozzan, T. (2008) *Proc. Natl. Acad. Sci. U.S.A.* **105,** 2859–2864
11. Large, W. A. (2002) *J. Cardiovasc. Electrophysiol.* **13,** 493–501
12. Yao, X., and Garland, C. J. (2005) *Circ. Res.* **97,** 853–863
13. Nakayama, H., Wilkin, B. J., Bodi, I., and Molkentin, J. D. (2006) *FASEB J.* **20,** 1660–1670
14. Kuwahara, K., Wang, Y., McAnally, J., Richardson, J. A., Bassel-Duby, R., Hill, J. A., and Olson, E. N. (2006) *J. Clin. Invest.* **116,** 3114–3126
15. Nishida, M., and Kurose, H. (2008) *Naunyn Schmiedebergs Arch. Pharmacology* **378,** 395–406
16. Bush, E. W., Hood, D. B., Papst, P. J., Chapo, J. A., Minobe, W., Bristow, M. R., Olson, E. N., and McKinsey, T. A. (2006) *J. Biol. Chem.* **281,** 33487–33496
17. Seth, M., Zhang, Z. S., Mao, L., Graham, V., Burch, J., Stiber, J., Tsiokas, L., Winn, M., Abramowitz, J., Rockman, H. A., Birnbaumer, L., and Rosenberg, P. (2009) *Circ. Res.* **105,** 1023–1030
18. Mori, Y., Wakamori, M., Miyakawa, T., Hermosura, M., Hara, Y., Nishida, M., Hirose, K., Mizushima, A., Kurosaki, M., Mori, E., Gotoh, K., Okada, T., Fleig, A., Penner, R., Iino, M., and Kurosaki, T. (2002) *J. Exp. Med.* **195,** 673–681
19. Zagranichnaya, T. K., Wu, X., and Villereal, M. L. (2005) *J. Biol. Chem.* **280,** 29559–29569
20. Hofmann, T., Schaefer, M., Schultz, G., and Gudermann, T. (2002) *Proc. Natl. Acad. Sci. U.S.A.* **99,** 7461–7466
21. Onohara, N., Nishida, M., Inoue, R., Kobayashi, H., Sumimoto, H., Sato, Y., Mori, Y., Nagao, T., and Kurose, H. (2006) *EMBO J.* **25,** 5305–5316
22. Kiyonaka, S., Kato, K., Nishida, M., Mio, K., Numaga, T., Sawaguchi, Y., Yoshida, T., Wakamori, M., Mori, E., Numata, T., Ishii, M., Takemoto, H., Ojida, A., Watanabe, K., Uemura, A., Kurose, H., Morii, T., Kobayashi, T., Sato, Y., Sato, C., Hamachi, I., and Mori, Y. (2009) *Proc. Natl. Acad. Sci. U.S.A.* **106,** 5400–5405
23. Hisatsune, C., Kuroda, Y., Nakamura, K., Inoue, T., Nakamura, T., Michikawa, T., Mizutani, A., and Mikoshiba, K. (2004) *J. Biol. Chem.* **279,** 18887–18894
24. Vazquez, G., Wedel, B. J., Kawasaki, B. T., Bird, G. S., and Putney, J. W., Jr.

(2004) *J. Biol. Chem.* **279,** 40521–40528
25. Kwan, H. Y., Huang, Y., and Yao, X. (2004) *Proc. Natl. Acad. Sci. U.S.A.* **101,** 2625–2630
26. Kass, D. A., Champion, H. C., and Beavo, J. A. (2007) *Circ. Res.* **101,** 1084–1095
27. Fiedler, B., Lohmann, S. M., Smolenski, A., Linnemuller, S., Pieske, B., Schroder, F., Molkentin, J. D., Drexler, H., and Wollert, K. C. (2002) *Proc. Natl. Acad. Sci. U.S.A.* **99,** 11363–11368
28. Takahashi, S., Lin, H., Geshi, N., Mori, Y., Kawarabayashi, Y., Takami, N., Mori, M. X., Honda, A., and Inoue, R. (2008) *J. Physiol.* **586,** 4209–4223
29. Takimoto, E., Champion, H. C., Li, M., Belardi, D., Ren, S., Rodriguez, E. R., Bedja, D., Gabrielson, K. L., Wang, Y., and Kass, D. A. (2005) *Nat. Med.* **11,** 214–222
30. Hsu, S., Nagayama, T., Koitabashi, N., Zhang, M., Zhou, L., Bedja, D., Gabrielson, K. L., Molkentin, J. D., Kass, D. A., and Takimoto, E. (2009) *Cardiovasc. Res.* **81,** 301–309
31. Lewis, G. D., Lachmann, J., Camuso, J., Lepore, J. J., Shin, J., Martinovic, M. E., Systrom, D. M., Bloch, K. D., and Semigran, M. J. (2007) *Circulation* **115,** 59–66
32. Takimoto, E., Koitabashi, N., Hsu, S., Ketner, E. A., Zhang, M., Nagayama, T., Bedja, D., Gabrielson, K. L., Blanton, R., Siderovski, D. P., Mendelsohn, M. E., and Kass, D. A. (2009) *J. Clin. Invest.* **119,** 408–420
33. Nishida, M., Maruyama, Y., Tanaka, R., Kontani, K., Nagao, T., and Kurose, H. (2000) *Nature* **408,** 492–495
34. Nishida, M., Onohara, N., Sato, Y., Suda, R., Ogushi, M., Tanabe, S., Inoue, R., Mori, Y., and Kurose, H. (2007) *J. Biol. Chem.* **282,** 23117–23128
35. Nishida, M., Sugimoto, K., Hara, Y., Mori, E., Morii, T., Kurosaki, T., and Mori, Y. (2003) *EMBO J.* **22,** 4677–4688
36. Nishida, M., Tanabe, S., Maruyama, Y., Mangmool, S., Urayama, K., Nagamatsu, Y., Takagahara, S., Turner, J. H., Kozasa, T., Kobayashi, H., Sato, Y., Kawanishi, T., Inoue, R., Nagao, T., and Kurose, H. (2005) *J. Biol. Chem.* **280,** 18434–18441
37. Nishida, M., Sato, Y., Uemura, A., Narita, Y., Tozaki-Saitoh, H., Nakaya, M., Ide, T., Suzuki, K., Inoue, K., Nagao, T., and Kurose, H. (2008) *EMBO J.* **27,** 3104–3115
38. Higazi, D. R., Fearnley, C. J., Drawnel, F. M., Talasila, A., Corps, E. M., Ritter, O., McDonald, F., Mikoshiba, K., Bootman, M. D., and Roderick, H. L. (2009) *Mol. Cell* **33,** 472–482
39. Dietrich, A., Mederos y Schnitzler, M., Emmel, J., Kalwa, H., Hofmann, T., and Gudermann, T. (2003) *J. Biol. Chem.* **278,** 47842–47852
40. Huang, J., Zhou, H., Mahavadi, S., Sriwai, W., and Murthy, K. S. (2007) *Am. J. Physiol. Cell Physiol.* **292,** C200–C208
41. Tokudome, T., Kishimoto, I., Horio, T., Arai, Y., Schwenke, D. O., Hino, J., Okano, I., Kawano, Y., Kohno, M., Miyazato, M., Nakao, K., and Kangawa, K. (2008) *Circulation* **117,** 2329–2339
42. Mederos y Schnitzler, M., Storch, U., Meibers, S., Nurwakagari, P., Breit, A., Essin, K., Gollasch, M., and Gudermann, T. (2008) *EMBO J.* **27,** 3092–3103
43. Inoue, R., Jensen, L. J., Jian, Z., Shi, J., Hai, L., Lurie, A. I., Henriksen, F. H., Salomonsson, M., Morita, H., Kawarabayashi, Y., Mori, M., Mori, Y., and Ito, Y. (2009) *Circ. Res.* **104,** 1399–1409
44. Gottlieb, P., Folgering, J., Maroto, R., Raso, A., Wood, T. G., Kurosky, A., Bowman, C., Bichet, D., Patel, A., Sachs, F., Martinac, B., Hamill, O. P., Honoré, E. (2008) *Pflugers Arch.* **455,** 1097–1103
45. Dietrich, A., Mederos Y Schnitzler, M., Gollasch, M., Gross, V., Storch, U., Dubrovska, G., Obst, M., Yildirim, E., Salanova, B., Kalwa, H., Essin, K., Pinkenburg, O., Luft, F. C., Gudermann, T., and Birnbaumer, L. (2005) *Mol. Cell. Biol.* **25,** 6980–6989
46. Trebak, M., Vazquez, G., Bird, G. S., and Putney, J. W., Jr. (2003) *Cell Calcium* **33,** 451–461

EXPERIMENTAL MEDICINE
実験医学 増刊

別　刷

羊土社
〒101-0052
東京都千代田区神田小川町2-5-1
TEL 03(5282)1211　FAX 03(5282)1212
E-mail：eigyo@yodosha.co.jp
URL：http://www.yodosha.co.jp/